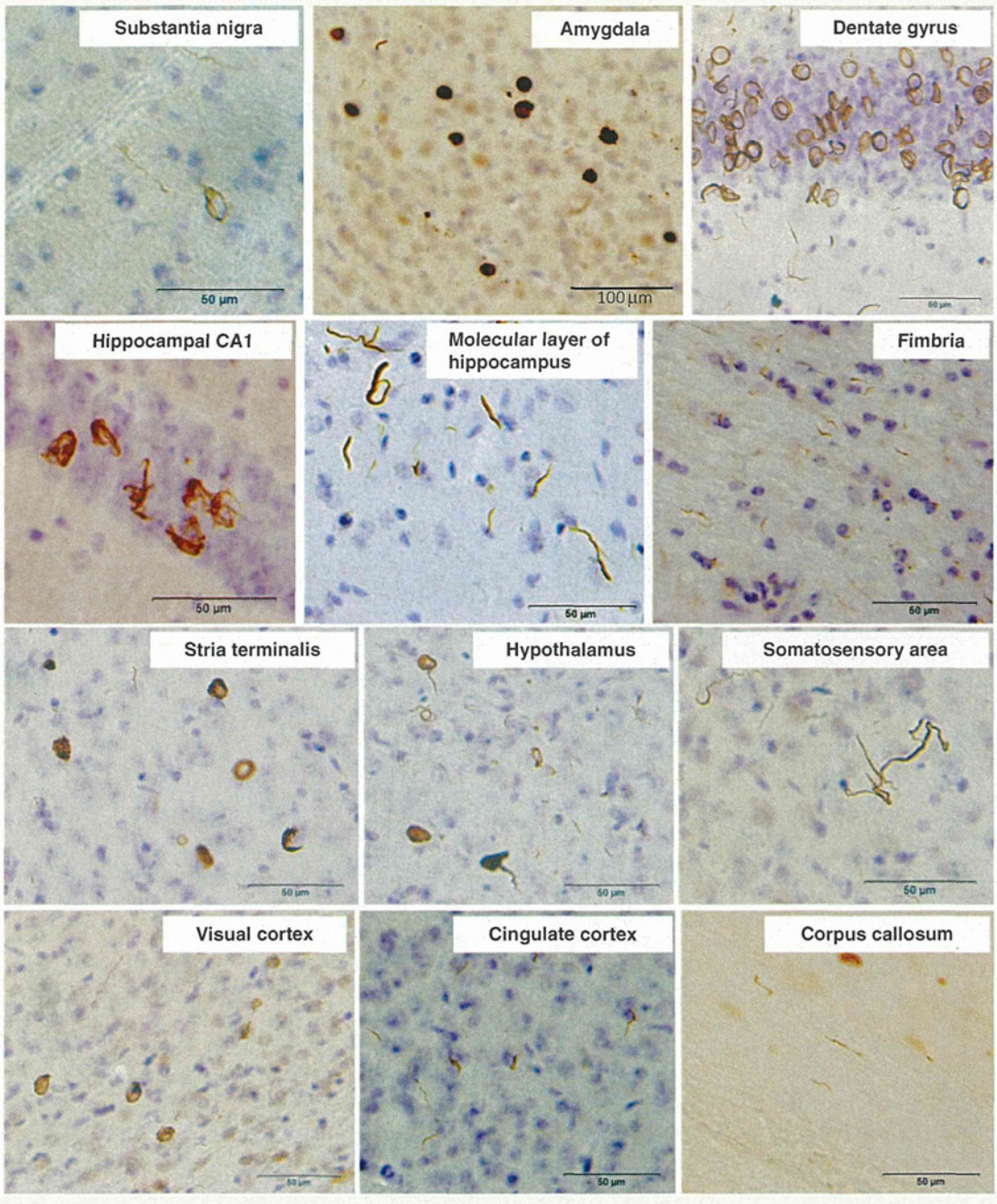

Figure 1 Induction of phosphorylated α-synuclein pathology in wild-type mouse brain injected with human α-synuclein fibrils, observed at 15 months after injection. Sections were immunostained with anti-phosphorylated α-synuclein antibody, 1175. The shapes of phosphorylated α-synuclein-positive structures differed among brain areas. Ring-like and Lewy neurite-like structures were observed in substantia nigra, hippocampus, hypothalamus, somatosensory area, visual cortex, cingulate cortex and corpus callosum, whereas Lewy body- and Lewy neurite-like structures were observed in amygdala and stria terminalis.

hours after injection (Day 0), injected recombinant human α-synuclein fibrils were detected in the sarkosyl-insoluble fraction of the right and left hemispheres by LB509 antibody, suggesting that injected human α-synuclein fibrils in the extracellular space spread quickly throughout the brain. However, at 7 days after injection, the human α-synuclein immunoreactivities had disappeared, and did not reappear at 30 or 90 days after injection (Fig. 4). At 90 days after injection, anti-phosphorylated α-synuclein-positive 15, 20, 30 and 35 kDa bands were detected in the sarkosyl-insoluble fractions. This band pattern is indistinguishable from that of pathological α-synuclein in dementia with Lewy bodies brain (Fig. 4). The 15, 20, 30 and 35 kDa bands correspond to α-synuclein monomer, mono-ubiquitinated α-synuclein, dimer and ubiquitinated dimer, respectively. Most

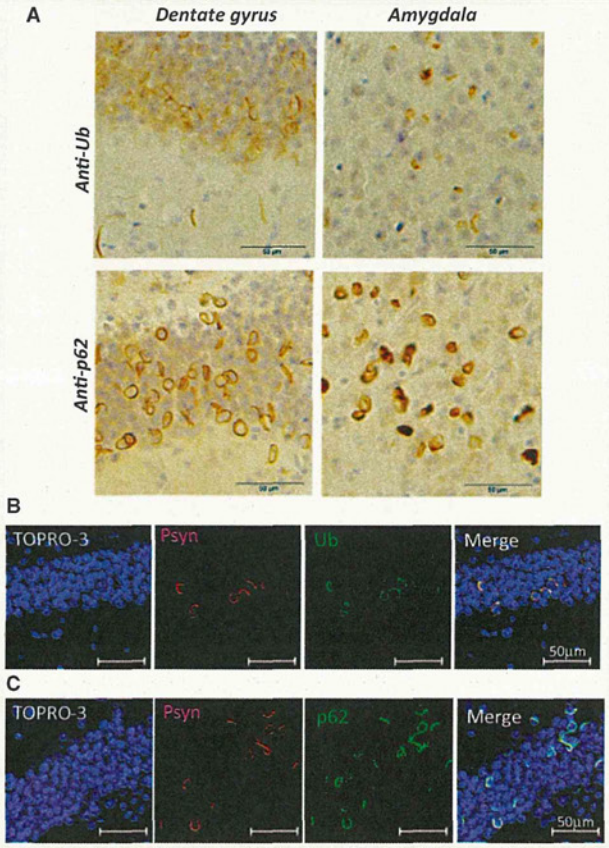

Figure 2 α-Synuclein pathology in fibril-injected mice brain was immunoreactive for ubiquitin (Ub) and p62. (**A**) Staining of dentate gyrus and amygdala of fibril-injected mice at 15 months after injection, using anti-ubiquitin (*upper*) and p62 (*lower*) antibodies. Abundant ubiquitin- and p62-positive pathology can be seen. (**B** and **C**) Double-labelled immunofluorescence of dentate gyrus for phosphorylated α-synuclein (Psyn) and ubiquitin (**B**) or p62 (**C**). Phosphorylated α-synuclein-positive structures were co-localized with ubiquitin and p62.

interestingly, anti-mouse α-synuclein strongly labelled the sarkosyl-insoluble phosphorylated α-synuclein-positive bands at Day 90, but these were not immunostained with LB509. These results clearly show that endogenous mouse α-synuclein is accumulated as phosphorylated and ubiquitinated forms. Immunohistochemical analysis with anti-tyrosine hydroxylase suggested that dopaminergic neurons are retained in substantia nigra of human α-synuclein fibril-injected mice at 6 months after injection (Fig. 5A and B). However, dramatic loss of the neurotransmitter enkephalin was observed in globus pallidus and amygdala central nucleus, where abundant phosphorylated α-synuclein-positive structures are detected (Fig. 5C and D). These data suggest that neuronal dysfunction occurs without apparent neuronal loss. We also performed behavioural analyses of mice injected with soluble human α-synuclein monomers or human α-synuclein fibrils. However, significant differences were not observed in open field test, wire hang test, rotarod test and Y-maze test (Supplementary Fig. 4) at 6 months after injection.

Next, we tested whether fibrils composed of recombinant mouse α-synuclein can induce α-synuclein pathology more efficiently than those composed of human α-synuclein, because the sequences of human and mouse α-synuclein are slightly different (Supplementary Fig. 5), and there could be a species difference. Mouse α-synuclein complementary DNA was cloned, and the protein was expressed in *Escherichia coli* and purified. Fibrils or soluble mouse α-synuclein were inoculated into substantia nigra of wild-type mouse brains and the pathology was evaluated. Strikingly, all the mice injected with mouse α-synuclein fibrils developed phosphorylated α-synuclein pathology in the injected side of the brain, whereas no pathology was detected in mice injected with soluble mouse α-synuclein (Table 2). The phosphorylated α-synuclein pathologies were basically the same as those of mice injected with human α-synuclein fibrils (data not shown). The efficiency of the induction of phosphorylated α-synuclein pathology by human α-synuclein fibrils was ~90% (Table 2), which is quite high, but slightly lower than that with mouse α-synuclein fibrils, suggesting that there may be a small species difference between mouse and human α-synuclein.

Finally, we tested whether pathological α-synuclein deposited in the brains of patients has similar prion-like properties in brains of wild-type mice. Surprisingly, pathological α-synuclein-enriched fractions also induced phosphorylated α-synuclein-positive pathologies in various areas of brain, including the substantia nigra, amygdala, hippocampus, striatum, hypothalamus, somatosensory area, motor cortex, piriform cortex and superior colliculus (Fig. 6). In brains of these mice, the phosphorylated α-synuclein-positive pathologies mostly resembled Lewy neurite-like structures. Lewy body-like pathology was detected only in amygdala and piriform cortex. The percentage of mice that developed phosphorylated α-synuclein pathology in the injected side of the brains was 50% in the group injected with insoluble phosphorylated α-synuclein of dementia with Lewy bodies brains, which is less than that in mice injected with recombinant α-synuclein fibrils (Table 2). Thus, these results demonstrate that inoculation of either pure synthetic recombinant α-synuclein fibrils or dementia with Lewy bodies brain extracts into wild-type mice can induce Lewy body/neurite-like phosphorylated α-synuclein pathology efficiently and reproducibly. Our results raise an important question, i.e. whether or not α-synuclein fibrils are transmissible among individuals. To test this possibility, we intranasally administered at high concentrarion of abnormal α-synuclein fibrils (preformed recombinant human or mouse α-synuclein fibrils) or the insoluble fraction from dementia with Lewy bodies brain to normal mice. However, no pS129-positive abnormal structures were detected in the brain at 21 months after the final administration (Supplementary Fig. 6), even with highly sensitive immunohistochemical staining, suggesting that the abnormal α-synuclein cannot pass through the nasal mucosa.

Discussion

In this study, we have shown that the inoculation of α-synuclein fibrils made of recombinant α-synuclein or dementia with Lewy bodies brain extracts into wild-type mouse brain is sufficient to

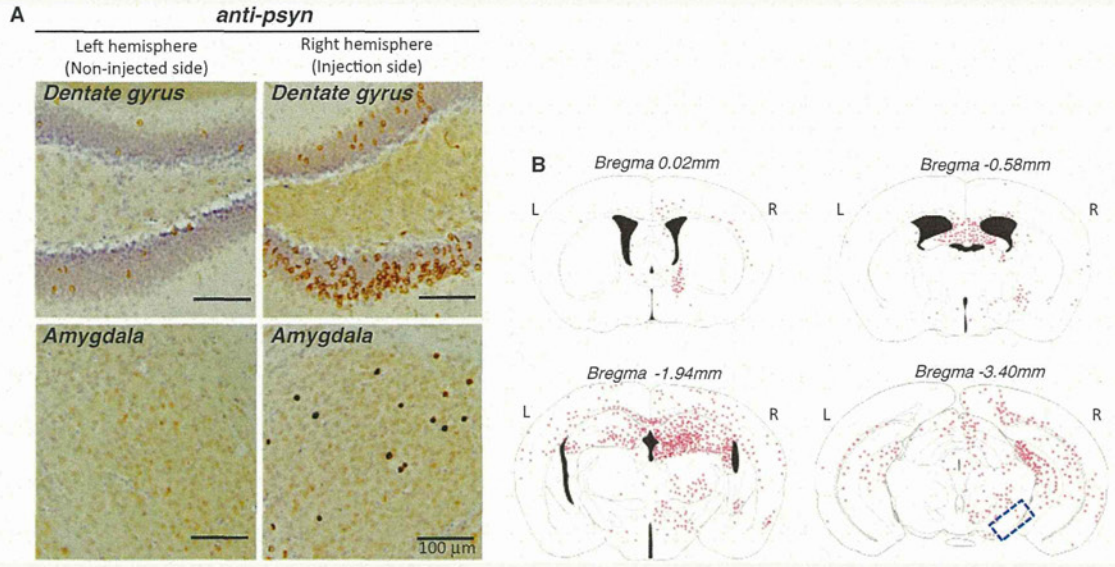

Figure 3 (**A**) Spreading of phosphorylated α-synuclein pathology on the contralateral side of mouse brain injected with α-synuclein fibrils. Staining of dentate gyrus and amygdala in the right hemisphere (injection side) and in the left hemisphere (non-injected side) with anti-phosphorylated α-synuclein (psyn) antibody, 1175, at 15 months after injection. (**B**) Distribution of phosphorylated α-synuclein pathology in human α-synuclein fibril-injected mouse brain at 15 months after injection ($n = 24$). Four coronal sections were stained with phosphorylated α-synuclein antibody, 1175. Red dots indicates Lewy bodies- and Lewy neurites-like pathology. Near the injection level (bregma -3.40 mm), abundant phosphorylated α-synuclein pathology was present in substantia nigra, hippocampus, external capsule, and entorhinal cortex in right hemisphere, whereas in the left hemisphere, sparser pathology was detected in hippocampus and external capsule. At the level of -1.94 mm from bregma, severe phosphorylated α-synuclein pathology was present in hippocampus, amygdala, corpus callosum, hypothalamus and motor, visual, somatosensory, auditory and piriform cortex in the right hemisphere, whereas moderate phosphorylated α-synuclein pathology was observed in corpus callosum, hippocampus, external capsule and motor, somasosensory and auditory cortex in the left hemisphere. At the level of -0.58 mm from bregma, phosphorylated α-synuclein pathology was detected in amygdala, corpus callosum, fimbria, fornix, hypothalamus, striatum and somatosensory and piriform cortex in the right hemisphere, whereas in the left hemisphere, the pathology was present in corpus callosum, fimbria, fornix, hypothalamus and striatum. At the level of 0.02 mm from bregma, phosphorylated α-synuclein pathology was concentrated in stria terminalis, septal nucleus and cingulate, motor and somatosensory cortex in the right hemisphere. In the left hemisphere, phosphorylated α-synuclein pathology was detected only in septal nucleus. Dashed box indicates substantia nigra (injection site). L = left hemisphere of brain; R = right hemisphere.

cause the appearance of Lewy body/neurite-like α-synuclein pathology *in vivo*. Similar work was recently published by Luk *et al.* (2012*a*) but there are important differences between our study and theirs. Luk *et al.* (2012*a*) showed that only inoculation of synthetic mouse α-synuclein fibrils into wild-type mouse brain induced synuclein pathology. In our present study, we inoculated not only fibrils made of recombinant mouse α-synuclein but also ones from human α-synuclein fibrils, and importantly also insoluble α-synuclein from dementia with Lewy bodies brains, into wild-type mouse brain. This is the first report showing efficient induction of α-synuclein pathology by inoculation of material from human brain. Furthermore, our biochemical analyses clearly demonstrate that endogenous mouse α-synuclein is converted into abnormal form and deposited in neurons of the brain through a prion-like mechanism or by seed-dependent aggregation by crossing the species barrier (Fig. 4). Since soluble α-synuclein never induced such pathology (Supplementary Fig. 2), we can conclude that the structural difference between soluble and filamentous forms of α-synuclein, i.e. cross-β structure in the α-synuclein fibrils (Serpell *et al.*, 2000) is critical for the pathogenesis. It has been reported that recombinant α-synuclein fibrils enhance the initiation and progression of α-synuclein pathology in transgenic mice overexpressing mutant α-synuclein (Mougenot *et al.*, 2012; Luk *et al.*, 2012*b*) and wild-type mice (Luk *et al.*, 2012*a*). In those models, α-synuclein pathology appeared at 90 days after inoculation. In our mouse model, abnormal phosphorylated α-synuclein pathology was also detected at 90 days after injection (Fig. 4 and Table 1), suggesting that it takes about this length of time for the formation of abnormal phosphorylated α-synuclein pathology *in vivo* after the seeding procedure. Despite a diffusion of injected exogenous α-synuclein fibrils to the bilateral sides of brain within a few hours after injection (Fig. 4), phosphorylated α-synuclein pathology seems to be initiated in the injected side and to spread from the injected side to the non-injected side in a time-dependent manner (Table 1). Thus, it is reasonable to speculate that exogenous fibrils enter neurons at the injection site as a result of infusion pressure, a temporary high concentration, or some other mechanism, and then the pathological process starts to develop from these cells.

Propagation patterns of pathology in the inoculated mice were basically identical regardless of the species of injected seeds (i.e. recombinant human α-synuclein fibrils, mouse α-synuclein fibrils or

Table 1 Semi-quantitative grading of α-synuclein pathology in mice injected with human α-synuclein fibrils

			Non-injection side (left hemisphere)			Injection side (right hemisphere)		
			Time from injection (days)			Time from injection (days)		
			90	180	450	90	180	450
Bregma	0.02 mm	Stria terminalis	−	−	−	−	+ +	+ + +
		Striatum	−	+	+	+	+ +	+ +
		Cigular cortex	−	−	−	−	+	+
		Septal nucleus	−	−	−	−	+	+
Bregma	−0.58 mm	Corpus callosum	−	−	+	−	−	+ +
		Fornix	−	+	+ +	−	+	+ +
		Hippocampal commissure	−	+	+ +	−	+	+ +
		Amygdala	−	−	−	+	+ + +	+ + +
		Globus pallidus	−	+	+	−	+	+ +
		Striatum	−	−	+	+	+	+
		Somatosensory area	−	−	+	−	+	+
		Insular cortex	−	−	−	+	+	+
Bregma	−1.94 mm	Corpus callosum	−	−	+ +	−	−	+ +
		Hippocampus	−	+	+ + +	+	+ +	+ + +
		Habenular nucleus	−	−	+	−	−	+ + +
		Fimbria	−	+	+ + +	−	+	+ + +
		Amygdala	−	−	−	+ +	+ + +	+ + +
		Hypothalamus	−	−	+	+	+	+ +
		Thalamus	−	−	−	−	−	+
		Visual cortex	−	−	+	−	+	+ +
		Somatosensory area	−	+	+	−	+	+ +
		Auditory cortex	−	−	+	+	+	+ +
		Piriform cortex	−	−	+	+	+	+ +
		External cupsule	−	−	+	−	−	+ +
Bregma	−3.40 mm	Substantia nigra	−	−	−	+	+	+
		Hippocampus	−	+	+ +	+	+ +	+ +
		Superior colliculus	−	+	+	−	+	+ +
		External cupsule	−	−	+	−	−	+
		Visual cortex	−	−	−	+	+	+
		Auditory cortex	+	+	+	+	+ +	+ +
		Entorhinal cortex	−	+	+	+	+ +	+ +

Four coronal sections were stained with anti-phosphorylated α-synuclein antibody at 90, 180 or 450 days after injection. Grading of α-synuclein pathology was performed as follows: −, none; +, slight; + +, moderate; + + +, severe. At 90 days after injection, small amounts of phosphorylated α-synuclein-positive structures were observed in substantia nigra, amygdala, striatum, hypothalamus, hippocampus, and stria terminalis in the right hemisphere of brain (injected side), but very few Lewy neurites were detected in cortex in the left hemisphere. At 180 days post-injection, the amount of phosphorylated α-synuclein-positive pathology was increased and was more widely spread in the right hemisphere, while in the left hemisphere, little phosphorylated α-synuclein pathology was apparent in hypothalamus, hippocampus, striatum or globus pallidus. At 450 days (15 months) after injection, phosphorylated α-synuclein pathology had spread throughout the right hemisphere and the left hemisphere.

dementia with Lewy bodies brain extracts), but extracts of brains with dementia with Lewy bodies showed lower propagation efficiency than recombinant fibrils (Table 2). This relatively low efficiency may be explained by the lesser amount of abnormal α-synuclein contained in the dementia with Lewy bodies brain extracts. Comparison of human α-synuclein fibrils and mouse α-synuclein fibrils indicated that mouse α-synuclein fibrils showed slightly higher efficiency (Table 2). *In vitro* experiments also indicated that mouse α-synuclein fibrils promote fibrillization of the soluble mouse α-synuclein monomer faster than human α-synuclein fibrils (Supplementary Fig. 7). It is well known that prion propagation can cross the species barrier (Prusiner, 1993) and the efficiency of propagation depends on the amino acid sequences of prion proteins. In the case of α-synuclein, mouse α-synuclein and human α-synuclein share 95% amino acid sequence homology (Supplementary Fig. 5), and this may be the reason why endogenous mouse α-synuclein is capable of aggregation by inoculation of human α-synuclein fibrils. Another factor may be that mouse α-synuclein protein has a threonine residue at amino acid position 53 (Supplementary Fig. 5), which is known as an aggregation-prone mutation in familial Parkinson's disease (Polymeropoulos *et al.*, 1997).

Time course analyses of the pathology in these mice (Table 1) showed that at 90 days after injection, phosphorylated α-synuclein pathology was mainly observed near the injection level, but also seen in striatum, amygdala, stria terminalis and dentate gyrus: areas far from the injection site had developed pathology. The striatum and the amygdala central nucleus have projections from substantia nigra, and the stria terminalis serves as a major output pathway of the amygdala (Supplementary Fig. 8). Although the

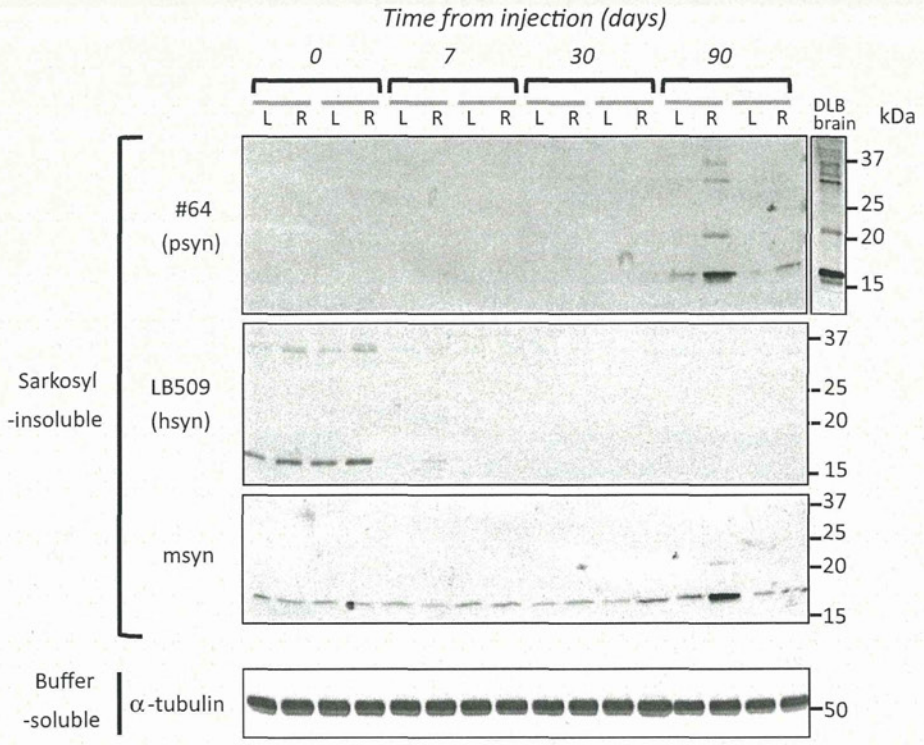

Figure 4 Endogenous mouse α-synuclein was aggregated in wild-type mouse brain injected with human α-synuclein (hsyn) fibrils. The brain was divided into two parts at the longitudinal fissure of the cerebrum. Sarkosyl-insoluble fractions were obtained from the right and left hemispheres, and analysed by immunoblotting with #64, LB509 or anti-mouse α-synuclein (msyn) antibodies. Representative images are shown (n = 14). Sarkosyl-insoluble phosphorylated α-synuclein (psyn) started to accumulate, predominantly in the right hemisphere, at 90 days after injection. It was composed of endogenous mouse α-synuclein, not exogenous human α-synuclein.

dentate gyrus does not have direct projection to substantia nigra, regions connecting with dentate gyrus (i.e., hippocampal CA1, CA3, entorhinal cortex, fimbria, fornix and hippocampal commissure) also showed moderate pathology (Table 1). These results may indicate that α-synuclein pathology propagates unidirectionally through the neural circuit (Supplementary Fig. 8). Spread of pathology from the right hemisphere to the left hemisphere might occur via the corpus callosum, hippocampal commissure, etc., connecting with the contralateral side of the brain (Fig. 3B and Table 1). Phosphorylated α-synuclein pathology in our mouse model was mainly observed in neurons and was hardly detected in glial cells, while the band pattern of sarkosyl-insoluble phosphorylated α-synuclein in mice was indistinguishable from that of dementia with Lewy bodies brains (Fig. 4), where phosphorylated α-synuclein pathology was mainly seen in neurons. Although the mechanism remains to be clarified, exogenous α-synuclein fibrils may enter cells through a selective mechanism(s), such as neuron-specific receptors. Alternatively, differences in expression levels of endogenous α-synuclein or cellular environments may also be important for formation of the pathology, even if abnormal α-synuclein has already entered the cells.

Luk *et al.* (2012a) reported dopaminergic neuronal loss and motor dysfunction (by Rotarod test and wire hang test) in wild-type mice injected with mouse α-synuclein fibrils at 6 months after inoculation into striatum. In contrast, our human α-synuclein or mouse α-synuclein fibril-injected mice did not

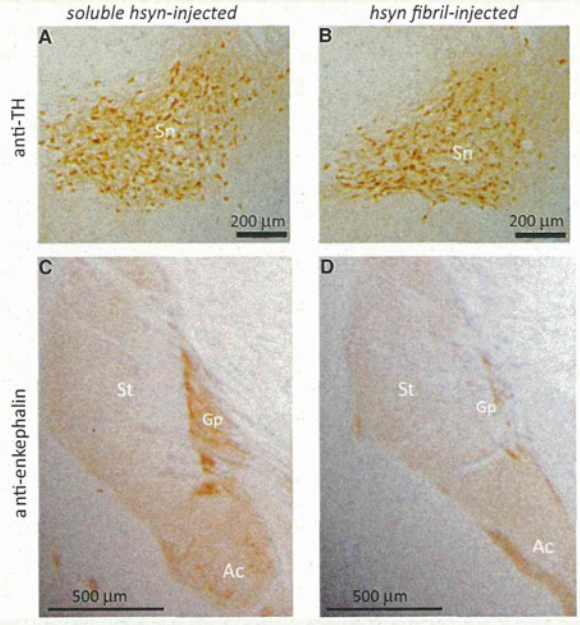

Figure 5 Fibril-injected mice show apparent reduction of a neurotransmitter enkephalin in amygdala central nucleus and globus pallidus at 15 months after injection. Brain sections were stained with anti-tyrosine hydroxylase (TH) (**A** and **B**) and anti-enkephalin (**C** and **D**) antibodies. Ac = amygdala central nucleus; Gp = globus pallidus; Sn = substantia nigra; St = striatum.

Table 2 Comparison of propagation efficiency in mice at 15 months after injection

Injection samples		Right hemisphere (injection side) anti-psyn	anti-ubiquitin	anti-p62	Left hemisphere (non-injected side) anti-psyn
Soluble human α-syn	(*n* = 8)	0/8 (0%)	0/8 (0%)	0/8 (0%)	0/8 (0%)
Insoluble human α-syn fibril	(*n* = 24)	22/24 (91.6%)	21/24 (87.5%)	22/24 (91.6%)	19/24 (79.2%)
Soluble mouse α-syn	(*n* = 4)	0/4 (0%)	0/4 (0%)	0/4 (0%)	0/4 (0%)
Insoluble mouse α-syn fibril	(*n* = 8)	8/8 (100%)	7/8 (87.5%)	8/8 (100%)	8/8 (100%)
DLB brain extracts	(*n* = 14)	7/14 (50%)	0/14 (0%)	5/14 (35.7%)	1/14 (7.1%)

In the right hemisphere, mice showing immunopositive structures for anti-phosphorylated α-synuclein (psyn), ubiquitin (Ub) or p62 were counted. In the left hemisphere, mice showing immunopositive structures for anti-phosphorylated α-synuclein were counted. Values show number of immunopositive mice/total mice, with percentage of immunopositive mice. DLB = dementia with Lewy bodies.

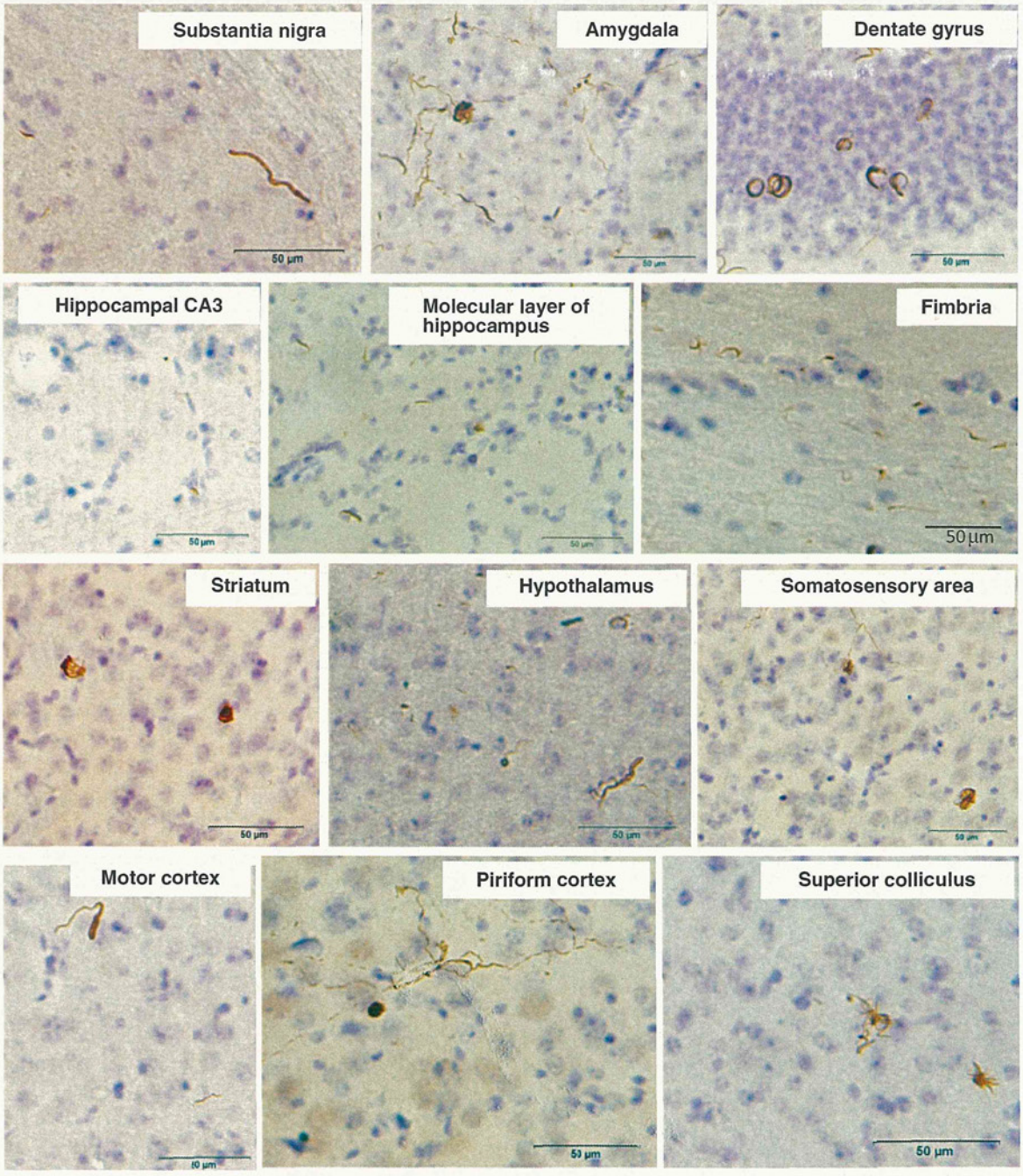

Figure 6 α-Synuclein pathology in wild-type mice brain injected with dementia with Lewy bodies-insoluble fraction observed at 15 months after injection. Sections were immunostained with anti-phosphorylated α-synuclein antibody, 1175.

show any motor and cognitive deficits at 6 months after inoculation and dopaminergic degeneration even after 15 months, a dramatic reduction of enkephalin was observed in the amygdala central nucleus and globus pallidus, with severe pathology, at 6 months after injection (Fig. 5 and Supplementary Fig. 4). The different phenotypes of these mice might be explained by differences in the injection sites [striatum in Luk *et al.* (2012*a*) and substantia nigra in our study]. Nonetheless, the spreading pattern of the pathological α-synuclein is different between our study and theirs. Differential vulnerability of neurons to these abnormal proteins may also affect phenotypes of these mice.

In summary, we have shown that intracerebral injection of insoluble α-synuclein fibrils can induce aggregation of endogenous mouse α-synuclein through a prion-like propagation mechanism. Our data suggest that phosphorylated α-synuclein pathologies do not induce acute neuronal loss but induce a slow neurodegeneration by disrupting neuronal function. These models should be useful not only for elucidating the molecular mechanisms of propagation of intracellular abnormal proteins, but also for development and evaluation of disease-modifying therapy.

Funding

This work was supported by MEXT KAKENHI Grant Numbers 12937622, 12901980 (to M.H.), JSPS KAKENHI Grant Number 11024780 (to M.M-S.) and MHLW Grant Number 12946221 (to M.H.).

Supplementary material

Supplementary material is available at *Brain* online.

References

Baba M, Nakajo S, Tu PH, Tomita T, Nakaya K, Lee VM, et al. Aggregation of alpha-synuclein in Lewy bodies of sporadic Parkinson's disease and dementia with Lewy bodies. Am J Pathol 1998; 152: 879–84.

Braak H, Braak E. Neuropathological stageing of Alzheimer-related changes. Acta Neuropathol 1991; 82: 239–59.

Chartier-Harlin MC, Kachergus J, Roumier C, Mouroux V, Douay X, Lincoln S, et al. Alpha-synuclein locus duplication as a cause of familial Parkinson's disease. Lancet 2004; 364: 1167–9.

Clavaguera F, Bolmont T, Crowther RA, Abramowski D, Frank S, Probst A, et al. Transmission and spreading of tauopathy in transgenic mouse brain. Nat Cell Biol 2009; 11: 909–13.

Desplats P, Lee HJ, Bae EJ, Patrick C, Rockenstein E, Crews L, et al. Inclusion formation and neuronal cell death through neuron-to-neuron transmission of alpha-synuclein. Proc Natl Acad Sci USA 2009; 106: 13010–5.

Emmanouilidou E, Melachroinou K, Roumeliotis T, Garbis SD, Ntzouni M, Margaritis LH, et al. Cell-produced alpha-synuclein is secreted in a calcium-dependent manner by exosomes and impacts neuronal survival. J Neurosci 2010; 30: 6838–51.

Fujiwara H, Hasegawa M, Dohmae N, Kawashima A, Masliah E, Goldberg MS, et al. Alpha-Synuclein is phosphorylated in synucleinopathy lesions. Nat Cell Biol 2002; 4: 160–4.

Goedert M. Alpha-synuclein and neurodegenerative diseases. Nat Rev Neurosci 2001; 2: 492–501.

Ibanez P, Bonnet AM, Debarges B, Lohmann E, Tison F, Pollak P, et al. Causal relation between alpha-synuclein gene duplication and familial Parkinson's disease. Lancet 2004; 364: 1169–71.

Kordower JH, Chu Y, Hauser RA, Freeman TB, Olanow CW. Lewy body-like pathology in long-term embryonic nigral transplants in Parkinson's disease. Nat Med 2008; 14: 504–6.

Kruger R, Kuhn W, Muller T, Woitalla D, Graeber M, Kosel S, et al. Ala30Pro mutation in the gene encoding alpha-synuclein in Parkinson's disease. Nat Genet 1998; 18: 106–8.

Kuusisto E, Salminen A, Alafuzoff I. Ubiquitin-binding protein p62 is present in neuronal and glial inclusions in human tauopathies and synucleinopathies. Neuroreport 2001; 12: 2085–90.

Li JY, Englund E, Holton JL, Soulet D, Hagell P, Lees AJ, et al. Lewy bodies in grafted neurons in subjects with Parkinson's disease suggest host-to-graft disease propagation. Nat Med 2008; 14: 501–3.

Luk KC, Kehm V, Carroll J, Zhang B, O'Brien P, Trojanowski JQ, et al. Pathological alpha-synuclein transmission initiates Parkinson-like neurodegeneration in nontransgenic mice. Science 2012a; 338: 949–53.

Luk KC, Kehm VM, Zhang B, O'Brien P, Trojanowski JQ, Lee VM. Intracerebral inoculation of pathological alpha-synuclein initiates a rapidly progressive neurodegenerative alpha-synucleinopathy in mice. J Exp Med 2012b; 209: 975–86.

Masuda M, Dohmae N, Nonaka T, Oikawa T, Hisanaga S, Goedert M, et al. Cysteine misincorporation in bacterially expressed human alpha-synuclein. FEBS Lett 2006a; 580: 1775–9.

Masuda M, Suzuki N, Taniguchi S, Oikawa T, Nonaka T, Iwatsubo T, et al. Small molecule inhibitors of alpha-synuclein filament assembly. Biochemistry 2006b; 45: 6085–94.

Mougenot AL, Nicot S, Bencsik A, Morignat E, Verchere J, Lakhdar L, et al. Prion-like acceleration of a synucleinopathy in a transgenic mouse model. Neurobiol Aging 2012; 33: 2225–8.

Muller CM, de Vos RA, Maurage CA, Thal DR, Tolnay M, Braak H. Staging of sporadic Parkinson disease-related alpha-synuclein pathology: inter- and intra-rater reliability. J Neuropathol Exp Neurol 2005; 64: 623–8.

Nonaka T, Kametani F, Arai T, Akiyama H, Hasegawa M. Truncation and pathogenic mutations facilitate the formation of intracellular aggregates of TDP-43. Hum Mol Genet 2009; 18: 3353–64.

Nonaka T, Watanabe ST, Iwatsubo T, Hasegawa M. Seeded aggregation and toxicity of {alpha}-synuclein and tau: cellular models of neurodegenerative diseases. J Biol Chem 2010; 285: 34885–98.

Polymeropoulos MH, Lavedan C, Leroy E, Ide SE, Dehejia A, Dutra A, et al. Mutation in the alpha-synuclein gene identified in families with Parkinson's disease. Science 1997; 276: 2045–7.

Prusiner SB. Genetic and infectious prion diseases. Arch Neurol 1993; 50: 1129–53.

Serpell LC, Berriman J, Jakes R, Goedert M, Crowther RA. Fiber diffraction of synthetic alpha-synuclein filaments shows amyloid-like cross-beta conformation. Proc Natl Acad Sci USA 2000; 97: 4897–902.

Shiotsuki H, Yoshimi K, Shimo Y, Funayama M, Takamatsu Y, Ikeda K, et al. A rotarod test for evaluation of motor skill learning. J Neurosci Methods 2010; 189: 180–5.

Singleton AB, Farrer M, Johnson J, Singleton A, Hague S, Kachergus J, et al. alpha-Synuclein locus triplication causes Parkinson's disease. Science 2003; 302: 841.

Spillantini MG, Crowther RA, Jakes R, Hasegawa M, Goedert M. alpha-Synuclein in filamentous inclusions of Lewy bodies from Parkinson's disease and dementia with lewy bodies. Proc Natl Acad Sci USA 1998; 95: 6469–73.

Spillantini MG, Schmidt ML, Lee VM, Trojanowski JQ, Jakes R, Goedert M. Alpha-synuclein in Lewy bodies. Nature 1997; 388: 839–40.

Stohr J, Watts JC, Mensinger ZL, Oehler A, Grillo SK, Dearmond SJ, et al. Purified and synthetic Alzheimer's amyloid beta (Abeta) prions. Proc Natl Acad Sci USA 2012; 109: 11025–30.

Volpicelli-Daley LA, Luk KC, Patel TP, Tanik SA, Riddle DM, Stieber A, et al. Exogenous alpha-synuclein fibrils induce Lewy body pathology leading to synaptic dysfunction and neuron death. Neuron 2011; 72: 57–71.

Wakabayashi K, Yoshimoto M, Tsuji S, Takahashi H. Alpha-synuclein immunoreactivity in glial cytoplasmic inclusions in multiple system atrophy. Neurosci Lett 1998; 249: 180–2.

Yonetani M, Nonaka T, Masuda M, Inukai Y, Oikawa T, Hisanaga S, et al. Conversion of wild-type alpha-synuclein into mutant-type fibrils and its propagation in the presence of A30P mutant. J Biol Chem 2009; 284: 7940–50.

Zarranz JJ, Alegre J, Gomez-Esteban JC, Lezcano E, Ros R, Ampuero I, et al. The new mutation, E46K, of alpha-synuclein causes Parkinson and Lewy body dementia. Ann Neurol 2004; 55: 164–73.

THE JOURNAL OF BIOLOGICAL CHEMISTRY VOL. 288, NO. 11, pp. 7968–7977, March 15, 2013

Isomerase Pin1 Stimulates Dephosphorylation of Tau Protein at Cyclin-dependent Kinase (Cdk5)-dependent Alzheimer Phosphorylation Sites*[S]

Received for publication, November 2, 2012, and in revised form, January 23, 2013 Published, JBC Papers in Press, January 28, 2013, DOI 10.1074/jbc.M112.433326

Taeko Kimura[‡], Koji Tsutsumi[‡], Masato Taoka[§], Taro Saito[‡], Masami Masuda-Suzukake[¶], Koichi Ishiguro[‖], Florian Plattner[**], Takafumi Uchida[‡‡], Toshiaki Isobe[§], Masato Hasegawa[¶], and Shin-ichi Hisanaga[‡1]

From the [‡]Laboratory of Molecular Neuroscience, Department of Biological Sciences, and [§]Department of Chemistry, Tokyo Metropolitan University, Hachioji, Tokyo 192-0397, Japan, [¶]Tokyo Metropolitan Institute of Medical Science, Setagaya, Tokyo 156-8506, Japan, [‖]Mitsubishi Kagaku Institute of Life Science, Machida, Tokyo 194-8511, Japan, [**]University of Texas Southwestern Medical Center, Dallas, Texas 75390-9070, and [‡‡]Department of Molecular Cell Biology, Graduate School of Agricultural Science, Tohoku University, Sendai, Miyagi 981-8555, Japan

Background: Hyperphosphorylated Tau is a component of neurofibrillary tangles, the pathological hallmark in brains with tauopathies.
Results: Pin1 binds phospho-Tau and stimulates its dephosphorylation at Cdk5-mediated phosphorylation sites.
Conclusion: Efficient Tau dephosphorylation at Alzheimer-related sites requires Pin1 activity, thereby preventing Tau hyperphosphorylation.
Significance: Disruption of Pin1-dependent facilitation of Tau dephosphorylation may be a critical mechanism underlying the etiology of tauopathies.

Neurodegenerative diseases associated with the pathological aggregation of microtubule-associated protein Tau are classified as tauopathies. Alzheimer disease, the most common tauopathy, is characterized by neurofibrillary tangles that are mainly composed of abnormally phosphorylated Tau. Similar hyperphosphorylated Tau lesions are found in patients with frontotemporal dementia with parkinsonism linked to chromosome 17 (FTDP-17) that is induced by mutations within the *tau* gene. To further understand the etiology of tauopathies, it will be important to elucidate the mechanism underlying Tau hyperphosphorylation. Tau phosphorylation occurs mainly at proline-directed Ser/Thr sites, which are targeted by protein kinases such as GSK3β and Cdk5. We reported previously that dephosphorylation of Tau at Cdk5-mediated sites was enhanced by Pin1, a peptidyl-prolyl isomerase that stimulates dephosphorylation at proline-directed sites by protein phosphatase 2A. Pin1 deficiency is suggested to cause Tau hyperphosphorylation in Alzheimer disease. Up to the present, Pin1 binding was only shown for two Tau phosphorylation sites (Thr-212 and Thr-231) despite the presence of many more hyperphosphorylated sites. Here, we analyzed the interaction of Pin1 with Tau phosphorylated by Cdk5-p25 using a GST pulldown assay and Biacore approach. We found that Pin1 binds and stimulates dephosphorylation of Tau at all Cdk5-mediated sites (Ser-202, Thr-205, Ser-235, and Ser-404). Furthermore, FTDP-17 mutant Tau (P301L or R406W) showed slightly weaker Pin1 binding than non-mutated Tau, suggesting that FTDP-17 mutations induce hyperphosphorylation by reducing the interaction between Pin1 and Tau. Together, these results indicate that Pin1 is generally involved in the regulation of Tau hyperphosphorylation and hence the etiology of tauopathies.

The neuropathological hallmarks of Alzheimer disease (AD)[2] include neurofibrillary tangles, which are composed mainly of abnormally phosphorylated microtubule-associated protein Tau (1). Aggregates of hyperphosphorylated Tau are also found in other neurodegenerative diseases that are collectively called tauopathies including Pick disease, progressive supranuclear palsy, corticobasal degeneration, and frontotemporal dementia with parkinsonism linked to chromosome 17 (FTDP-17) (2). FTDP-17 is an inherited form of tauopathy that is caused by mutations within the *tau* gene and is characterized by lesions containing hyperphosphorylated Tau (3–5). Genetically modified mice featuring the *tau* mutations of FTDP-17 developed similar aggregates of hyperphosphorylated Tau and showed dementia-like memory impairments, indicating a causative role of the *tau* mutations (2, 6, 7). However, it is not yet known why these Tau mutations induce Tau aggregation and neurodegeneration. Understanding the molecular mechanisms that induce Tau hyperphosphorylation and aggregation in AD and FTDP-17 may be critical to unravel the processes underlying the etiology of tauopathies.

Tau in neurofibrillary tangles is phosphorylated at more than 30 sites with most of them being located in the flanking regions of the microtubule-binding repeats (8–10). Many protein

* This work was supported in part by grants-in-aid for scientific research from the Ministry of Education, Culture, Sports, Science and Technology of Japan (to S. H.).
[S] This article contains supplemental Figs. 1–5.
[1] To whom correspondence should be addressed. Tel.: 81-42-677-2769; Fax: 81-42-677-2559; E-mail: hisanaga-shinichi@tmu.ac.jp.

[2] The abbreviations used are: AD, Alzheimer disease; Cdk, cyclin-dependent kinase; FTDP-17, frontotemporal dementia with parkinsonism linked to chromosome 17; Pin1, peptidyl-prolyl *cis/trans* isomerase, NIMA-interacting 1; GSK3β, glycogen synthase kinase 3β; PDPK, proline-directed protein kinase; PP2A, protein phosphatase 2A; Req, response at equilibrium; juglone, 5-hydroxy-1,4-naphthoquinone; CBB, Coomassie Brilliant Blue.

kinases have been implicated in Tau phosphorylation. Proline-directed protein kinases (PDPKs) such as glycogen synthase kinase 3β (GSK3β) and cyclin-dependent kinase 5 (Cdk5) have been thought to be critically involved in abnormal Tau phosphorylation because many proline-directed sites are hyperphosphorylated in Tau (2, 8, 10–12).

Cdk5, originally purified as Tau kinase II (13), is a serine/threonine kinase with pleiotropic functions in postmitotic neurons (14, 15). Cdk5 requires binding of the activation subunit, p35, for activation. The active holoenzyme Cdk5-p35 is localized to the cell membrane via the myristoylation of p35 (16–18). Membrane-associated Cdk5-p35 exhibits moderate kinase activity due to a short half-life of p35, which is degraded by the proteasome (19). Alternatively, p35 can be cleaved to p25 by calpain, and the Cdk5-p25 holoenzyme can subsequently relocalize to the cytoplasm and/or nucleus (16, 20, 21). The Cdk5 activator, p25, has a long half-life (16, 21) and induces aberrant Cdk5 activity toward Tau (22, 23). Consistently, silencing of Cdk5 reduced the phosphorylation of Tau in primary neuronal cultures and in brain and decreased the number of neurofibrillary tangles in the hippocampi of transgenic Alzheimer disease mice (24). However, it is not clear how Cdk5-p25 causes Tau hyperphosphorylation and aggregation.

In FTDP-17 patients and transgenic mouse models, Tau is hyperphosphorylated (2, 8, 10, 11, 25). In contrast, FTDP-17 mutant Tau is less phosphorylated than wild-type (WT) Tau *in vitro* or in cell cultures (26–29). These studies suggest that disruption of dephosphorylation rather than increased phosphorylation contributes to the hyperphosphorylated state of Tau. Accordingly, protein phosphatase 2A (PP2A) activity is decreased in AD brains (30–32), and highly phosphorylated Tau in paired helical filament is relatively resistant to dephosphorylation by PP2A (33). Furthermore, PP2A preferentially dephosphorylated phospho-(Ser/Thr)-Pro motifs in *trans* conformation when synthetic phospho-Thr-231 Tau peptide was used as a substrate (34, 35). Peptidyl-prolyl *cis/trans* isomerase, NIMA-interacting 1 (Pin1) is a peptidylprolyl isomerase composed of two functional domains, the N-terminal WW domain, which binds to phosphorylated Ser or Thr at proline-directed sites, and the C-terminal *cis/trans* isomerase domain (36, 37). Pin1 is found in neurofibrillary tangles, and Tau hyperphosphorylation is reported in Pin1-deficient mice (38). Hence, Pin1 could be a critical regulator of Tau dephosphorylation to (i) restore physiological Tau function such as microtubule binding and (ii) suppress neurofibrillary tangle formation by enhancing dephosphorylation by PP2A. We reported recently that Pin1 stimulates dephosphorylation of Tau phosphorylated by Cdk5-p25, suggesting that there are more Pin1 binding motifs in Tau (39). The Pin1 binding sites in Tau were shown to be phospho-Thr-231 (34, 40) and phospho-Thr-212 (41). However, these two Pin1 binding sites alone cannot prevent abnormal Tau phosphorylation at all the other hyperphosphorylation sites. Therefore, we wanted to assess Pin1 binding at additional Tau phosphorylation sites.

Here we analyzed interaction of Pin1 with Cdk5-mediated Tau phosphorylation sites using a GST pulldown assay and Biacore technique. We observed that Pin1 binds to Tau and stimulates its dephosphorylation at all Cdk5 phosphorylation sites including Ser-202, Thr-205, Ser-235, and Ser-404. Furthermore, Tau carrying the FTDP-17 mutation P301L or R406W showed slightly weaker binding to Pin1 than WT Tau, suggesting that FTDP-17 mutations induce Tau hyperphosphorylation by reducing its interaction with Pin1.

EXPERIMENTAL PROCEDURES

Antibodies and Chemicals—Anti-Pin1 and anti-actin were purchased from Santa Cruz Biotechnology (Santa Cruz, CA), anti-human Tau (A0024) was obtained from Dako Denmark (Glostrup, Denmark), anti-Tau Ab-2 (Tau5) was purchased from Thermo Fisher Scientific Anatomical Pathology (Fremont, CA), Tau-C was prepared as described previously (42), anti-phospho-Tau (Ser(P)-202, Thr(P)-205, and Ser(P)-404) was obtained from Invitrogen, and anti-phospho-Tau (Ser(P)-235) was from Abcam (Cambridge, UK). Goat anti-GST antibody was purchased from GE Healthcare. Phos-tag acrylamide and 4-(2-aminoethyl)-benzenesulfonyl fluoride hydrochloride (Pefabloc) were purchased from Wako Chemicals (Osaka, Japan). Leupeptin was obtained from the Peptide Institute (Osaka, Japan). 5-Hydroxy-1,4-naphthoquinone (juglone) and Dulbecco's modified Eagle's medium (DMEM) were from Sigma-Aldrich. HilyMax transfection reagent was from Dojindo Laboratories (Kumamoto, Japan).

Plasmid Construction of Mutant Tau—The 412-amino acid isoform (1N4R; containing one N-terminal insertion and four microtubule-binding repeats) of human Tau was used (29). Alanine mutants of Tau at Ser-202 (S202A), Thr-205 (T205A), Thr-212 (T212A), Thr-231 (T231A), or Ser-235 (S235A) were generated using 1N4R human *tau* as a template with the QuikChange site-directed mutagenesis kit (Stratagene, La Jolla, CA) according to the manufacturer's instructions. The primers used were as follows: 5′-GGGAGTGCCTGGGGCGCCGGGGCTGCT-3′ and 5′-AGCAGCCCCGGCGCCCCAGGCACTCCC-3′ for S202A, 5′-GCTCCCCAGGCGCTCCCGGCAGCCGCT-3′ and 5′-AGCGGCTGCCGGGAGCGCCTGGGGAGC-3′ for T205A, 5′-CAGCCGCTCCCGCGCCCCGTCCCTTCC-3′ and 5′-GGAAGGGACGGGGCGCGGGAGCGGCTG-3′ for T212A, 5′-GGCAGTGGTCCGTGCTCCACCCAAGTC-3′ and 5′-GACTTGGGTGGAGCACGGACCACTGCC-3′ for T231A, and 5′-TACTCCACCCAAGGCGCCGTCTTCCGC-3′ and 5′-GCGGAAGACGGCGCCTTGGGTGGAGTA-3′ for S235A. Ser-202, Thr-205, Ser-235, and Ser-404 were mutated to Ala in *Tau-4A* by PCR using the primers described above. Tau-3A mutants with a single phosphorylation site were constructed by adding back one of Ser-202, Thr-205, Ser-235, or Ser-404 to *Tau-4A*.

Expression and Purification of Recombinant Human Tau—Expression of recombinant human Tau (either the WT or Ala mutants) and FTDP-17 mutant Tau (P301L and R406W) was performed in *Escherichia coli* BL21-CodonPlus (DE3)-RP as described previously (29). Tau proteins were purified from heat-treated extracts using a Mono S column with an ÄKTA purifier (GE Healthcare). The amount of Tau protein was estimated by Coomassie Brilliant Blue (CBB) staining of gels using bovine serum albumin (BSA) as a standard.

Cloning, Mutant Construction, and Expression of Pin1—*Pin1* cDNA was amplified from an adult mouse brain cDNA library

by PCR using oligonucleotides 5′-GAATTCATGGCGGACG-AGGAGAAG-3′ and 5′-CTCGAGTCATTCTGTGCGCAG-GAT-3′ as the forward and reverse primers, respectively. GST-Pin1 was generated by inserting *Pin1* cDNA into EcoRI/Xho1 sites of pGEX4T-1 (GE Healthcare). Asp mutants of Pin1 at Tyr-23 (Y23D) and Trp-34 (W34D) were generated using mouse *Pin1* as a template with the QuikChange site-directed mutagenesis kit. The primers used were as follows: 5′-CAGG-CCGGGTGGACTACTTCAATCACA-3′ and 5′-TGTGATT-GAAGTAGTCCACCCGGCCTG-3′ for Y23D and 5′-CACC-AACGCCAGCCAGGACGAGCGGCCCAGCGGCG-3′ and 5′-CGCCGCTGGGCCGCTCGTCCTGGCTGGCGTTGGTG-3′ for W34D. GST-Pin1 or its mutants were expressed in the BL21 *E. coli* strain (DE3) and purified from the cell extract using GSH beads (GE Healthcare).

Preparation of Extracts from COS-7 Cells or Mouse or Human Brain—COS-7 cells were maintained in DMEM supplemented with 10% fetal bovine serum, 100 units/ml penicillin, and 0.1 mg/ml streptomycin. COS-7 cells were transfected with *p25*, *Cdk5*, *tau*, and/or *Pin1* expression plasmids by HilyMax transfection reagent (Dojindo Laboratories). Twenty-four hours after transfection, the cells were lysed in 20 mM HEPES, pH 7.4, 1 mM $MgCl_2$, 100 mM NaCl, 0.5% Nonidet P-40, 0.4 mM Pefabloc, 10 μg/ml leupeptin, and 1 mM dithiothreitol (DTT) on ice for 10 min. After centrifugation at 15,000 × *g* for 15 min, the supernatant was collected as a COS-7 cell extract. Four-week-old C57BL/6J mice were obtained from Sankyo Labo Service (Tokyo, Japan). Brain cortex was homogenized in 20 mM HEPES, pH 7.4, 100 mM NaCl, 0.1% Nonidet P-40, 2 mM $MgCl_2$, 1 mM EGTA, 0.4 mM Pefabloc, 10 μg/ml leupeptin, and 1 mM DTT. After centrifugation at 15,000 × *g* for 20 min, the supernatant was used as a brain extract. The extract was incubated with or without 1 mM ATP and/or 20 μM roscovitine (Calbiochem) at 35 °C for 1 h to induce phosphorylation of Tau. The human brain tissues were kindly provided by the University College London Queen Square Brain Bank (London, UK). Lysates were prepared from snap frozen human brain tissues from a male FTDP-17 patient and three male non-AD controls. Small frozen tissue samples were homogenized in ice-cold P2 buffer containing protease and phosphatase inhibitors as described previously (12).

Preparation of Cdk5-p25 from Sf9 Cells and Phosphorylation of Tau—Cdk5-p25 was purified from Sf9 cells infected by baculovirus encoding Cdk5 and p25 as described previously (43). Tau at 0.1 mg/ml was phosphorylated by Cdk5-p25 at 35 °C for 1.5 h in 10 mM MOPS, pH 6.8, 2 mM $MgCl_2$, 0.1 mM EDTA, 0.1 mM EGTA, 0.1% Nonidet P-40, and 1 mM ATP or 0.1 mM [γ-^{32}P]ATP. Phosphorylation was detected by autoradiography after SDS-PAGE on a 10% polyacrylamide gel, and the extent of Tau phosphorylation was quantified using a FLA7000 bioimage analyzer (Fujifilm, Tokyo, Japan). Two-dimensional phosphopeptide map analysis of phospho-Tau was performed as described previously (29).

GST Pulldown Assay—GST or GST-Pin1 was incubated with GSH-Sepharose 4B (GE Healthcare) at 4 °C for 1 h and then incubated with mouse brain extract or *E. coli* extract containing Tau at 4 °C for 2 h. The beads were washed five times with HEPES buffer (20 mM HEPES, pH 7.4, 100 mM NaCl, 2 mM $MgCl_2$, 0.5% Nonidet P-40, 1 mM EGTA, 10 mM NaF, 10 mM β-glycerophosphate, 1 mM Na_3VO_4, 10 μg/ml leupeptin, 0.2 mM Pefabloc, and 1 mM DTT), and the proteins bound to beads were eluted by boiling in SDS sample buffer.

Surface Plasmon Resonance Analysis of the Binding between Pin1 and Phosphorylated Tau—The affinity of phosphorylated Tau binding to Pin1 was measured with a Biacore 2000 surface plasmon resonance spectroscope (GE Healthcare) as described previously (44). Briefly, anti-GST antibody was immobilized on a CM5 sensor chip using an amine coupling kit (GE Healthcare) according to the manufacturer's protocol. All measurements were performed using 10 mM HEPES, pH 7.0, 100 mM NaCl, 1.5 mM EDTA, and 0.01% Nonidet P-40. Purified Tau was injected at a rate of 5 μl/min at 25 °C. For the kinetic analysis, various concentrations of Tau were loaded onto the sensor surface to equilibrate the Tau-Pin1 interaction, and the amount of the complex (the response at equilibrium (Req)) was measured in resonance units. The correlation between Req, the concentration of ligand (*C*) passed over the sensor surface, and the total binding capacity (R_{max}) of the immobilized protein was calculated as: $Req/C = K_aR_{max} - K_aReq$. The association constant (K_a) was determined from the plot of Req/*C versus* Req estimated at different Tau concentrations by Scatchard plot analysis. Statistical analysis was performed using a linear regression method.

SDS-PAGE, Phos-tag SDS-PAGE, and Immunoblotting—SDS-PAGE was performed according to the method of Laemmli (45) using a 12.5% polyacrylamide gel. Phos-tag SDS-PAGE was performed with 7.5% polyacrylamide gels containing 50 μM Phos-tag acrylamide and 150 μM $MnCl_2$ (46, 47). Proteins were transferred to a PVDF membrane using a submerged blotting system. The reaction was detected using an enhanced chemiluminescence detection kit (GE Healthcare).

RESULTS

Cdk5 Phosphorylation Is a Prerequisite for Pin1 Binding to Tau—We have reported previously that recombinant Tau phosphorylated by Cdk5-p35 is dephosphorylated by PP2A faster in WT mouse brain extract than in Pin1-deficient mouse brain extract (39). This result suggests that Pin1 recognizes Cdk5-phosphorylated Tau to stimulate its dephosphorylation. However, there has been no report describing Pin1 binding to Cdk5-mediated Tau phosphorylation sites. Therefore, we wanted to know whether endogenous Tau in mouse brain binds to Pin1. Tau was phosphorylated by incubation with ATP at 35 °C for 1 h in the presence or absence of the Cdk5 inhibitor roscovitine, and the binding of Tau to Pin1 was assessed using a GST-Pin1 pulldown assay. Incubation with ATP increased the amount of Tau bound to Pin1 more than 7-fold. In contrast, application of roscovitine decreased the amount of Tau bound to Pin1 by more than 30% (Fig. 1). These results suggest that Cdk5-mediated phosphorylation facilitates the binding of Tau to Pin1. Other Tau kinases (*e.g.* GSK3β) that phosphorylate Tau at similar sites may also increase the interaction between Tau and Pin1.

Pin1 Binds to Tau When Phosphorylated by Cdk5-p25 and GSK3β but Not by the Catalytic Subunit of cAMP-dependent Protein Kinase (PKA)—To demonstrate more conclusively that Pin1 can bind to Tau phosphorylated by Cdk5, recombinant

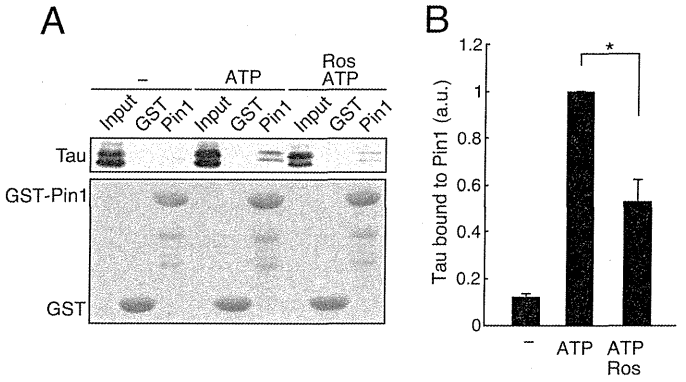

FIGURE 1. **Endogenous Tau phosphorylated by Cdk5 in mouse brain extracts binds to Pin1.** Mouse brain extract was incubated with ATP in the presence or absence of 20 μM roscovitine (*Ros*) at 35 °C for 1 h. The incubated extracts were subjected to a pulldown assay using GST-Pin1 (*Pin1*) or GST. *A*, the binding of Tau was detected by immunoblotting with anti-Tau antibody (Tau5) (*upper panel*). CBB staining of GST-Pin1 and GST is shown in the *lower panel*. *B*, quantification of Tau bound to GST-Pin1. The results are expressed as mean ± S.E. (*error bars*) ($n = 3$; *, $p < 0.05$). *a.u.*, arbitrary units.

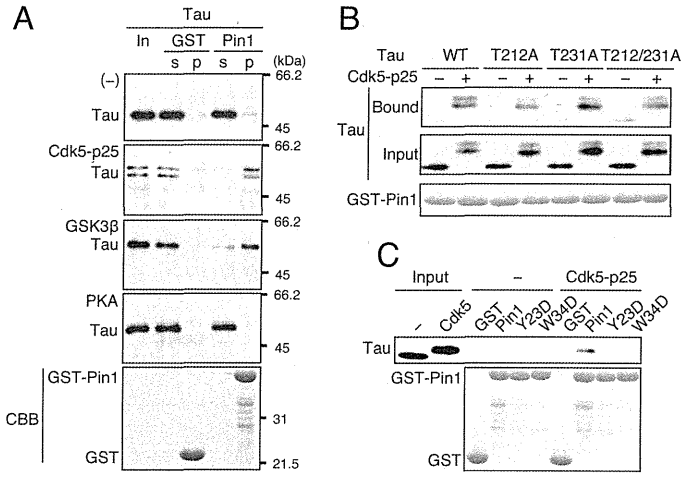

FIGURE 2. **Recombinant Tau phosphorylated *in vitro* by Cdk5-p25 or GSK3β, but not by PKA, binds to Pin1.** *A*, recombinant Tau phosphorylated by Cdk5-p25, GSK3β, or PKA was subjected to a GST-Pin1 pulldown assay. *s*, supernatant; *p*, pellet. Unphosphorylated Tau is shown in the *first panel* ([−]). Tau bound to GST-Pin1 was detected by immunoblotting with Tau5 (*first to fourth panels*). The input is shown in the lanes labeled "*In*." GST-Pin1 and GST are shown by CBB staining (*lower panel*). *B*, Tau binds to Pin1 at phosphorylation sites other than Thr-212 and Thr-231. Tau-T212A, Tau-T231A, or Tau-T212A/T231A was phosphorylated by Cdk5-p25 and subjected to the GST pulldown assay. Tau bound to Pin1 (*upper panel*) and in the input (*second panel*) was detected by immunoblotting with Tau5. CBB staining shows GST-Pin1 (*lower panel*). *C*, the WW domain-dependent binding of Pin1 to Cdk5-phosphorylated Tau. Unphosphorylated Tau (−) or Cdk5-phosphorylated Tau (Cdk5-p25) was subjected to the GST pulldown assay using an Asp mutant of Pin1 at Tyr-23 (Y23D) or Trp-34 (W34D) in the WW domain. *Input* shows unphosphorylated (−) and Cdk5-phosphorylated (*Cdk5*) Tau. CBB staining shows GST-Pin1 and GST (*lower panel*).

Tau was phosphorylated by Cdk5-p25 *in vitro*, and its binding to Pin1 was examined. Tau was also phosphorylated by GSK3β, another PDPK, and the PKA, a non-PDPK, and their binding to Pin1 was examined as a positive and negative control, respectively. Tau phosphorylated by Cdk5-p25 or GSK3β, but not by PKA, bound to GST-Pin1 (Fig. 2*A*). No binding was observed with control GST beads. These results indicate that Pin1 binds to Tau at proline-directed Ser/Thr phosphorylation sites that are modified by Cdk5 and GSK3β.

There are six isoforms of Tau in the human brain (48) that differ in the N-terminal insertion of exons 2 and/or 3 and in the C terminus of exon 10. The latter splicing produces Tau isoforms with three (3R) or four (4R) microtubule-binding repeats. The ratio of Tau 3R to 4R in neurofibrillary tangles differs between tauopathies (2, 49). We next examined whether individual Tau isoforms have distinct binding affinities for Pin1. All Tau isoforms bound to Pin1 after phosphorylation by Cdk5, and the binding did not differ between isoforms (supplemental Fig. 1). Therefore, we decided to use the Tau 1N4R isoform in the following experiments.

Pin1 Binds to Tau at Phosphorylation Sites Other than Thr-212 and Thr-231—It has been reported that Thr-212 and Thr-231 in Thr-Pro sequences are the Pin1-binding sites (40, 41). Thr-212 and Thr-231 are not major Cdk5-mediated phosphorylation sites (29); nevertheless, it is possible that these sites can be phosphorylated by Cdk5 *in vitro* and hence explain the increased Pin1 binding after Cdk5-mediated phosphorylation. To test this possibility, we generated mutant Tau in which the threonine residues at position 212 and/or 231 were replaced with non-phosphorylatable alanine (T212A, T231A, and T212A/T231A), and we examined the binding of the mutant Tau to GST-Pin1 after Cdk5 phosphorylation (Fig. 2*B*). The upward shift of Tau-T212A, Tau-T231A, and Tau-T212A/T231A was similar to that of WT Tau, suggesting that these sites are not efficiently phosphorylated by Cdk5. Consistently, an *in vitro* kinase assay revealed that the Tau mutants (T212A, T231A, and T212A/T231A) exhibited phosphorylation levels comparable with those of WT Tau (supplemental Fig. 2). All of these Ala mutants phosphorylated by Cdk5-p25 bound to Pin1 (Fig. 2*B*). The results suggest that Pin1 can bind to sites other than Thr-212 and Thr-231 in Cdk5-phosphorylated Tau. Pin1 binds to the phospho-(Ser/Thr)-Pro sequences via its N-terminal WW domain (36, 37). To confirm that Cdk5-phosphorylated Tau binds to Pin1 via the WW domain, we generated Asp or Trp mutants of Pin1 at the critical Tyr-23 residue (Pin1-Y23D) or Trp-34 residue (Pin1-W34D) in the WW domain, and we examined their binding to Cdk5-phosphorylated Tau. These Pin1 mutants did not bind to phosphorylated Tau (Fig. 2*C*), indicating that Pin1 binding to Cdk5-phosphorylated Tau is dependent on WW domain-mediated interaction.

The Major Cdk5 Phosphorylation Sites in Tau Are Ser-202, Ser-235, Ser-404, and Thr-205—The Cdk5 phosphorylation sites in Tau reported so far include Thr-153, Thr-181, Thr-199, Ser-202, Thr-205, Thr-212, Ser-214, Thr-231, Ser-235, Ser-396, and Ser-404 (8, 11, 29, 39, 50). Some of these sites may be minor sites that were identified with phosphorylation-specific antibodies. To identify Pin1-binding Cdk5 phosphorylation sites, we first needed to identify all major Cdk5 phosphorylation sites. We have previously identified the major Cdk5 phosphorylation sites in Tau as Ser-202, Ser-235, and Ser-404 biochemically using two-dimensional phosphopeptide mapping (29, 39, 51). However, there was ambiguity about Thr-205, which is included in the same tryptic peptide as Ser-202 (Fig. 2*A*, amino acid sequences shown between the domain structure of Tau and mutants). We then determined whether Thr-205 could also be phosphorylated by Cdk5-p25. Ala mutants of Tau at Ser-202, Thr-205, or both were phosphorylated by Cdk5-p25 (Fig. 3*B*) and then subjected to two-dimensional phosphopeptide map

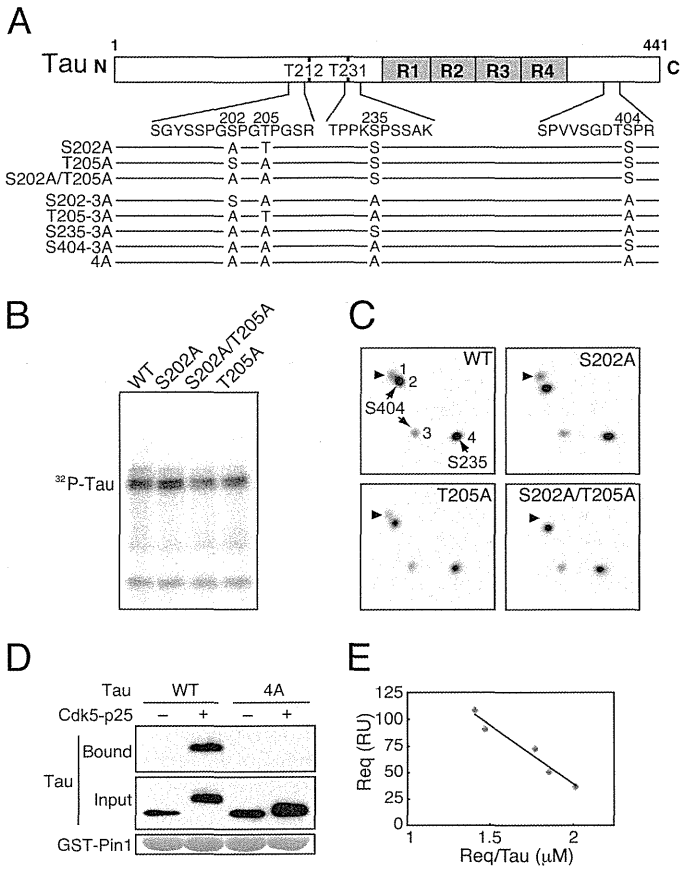

FIGURE 3. **Tau lacking four Cdk5 phosphorylation sites does not bind to Pin1.** *A*, domain structure and major Cdk5 phosphorylation sites in the longest human Tau comprising 441 amino acids. *R1–R4* are microtubule-binding repeats, and Thr-212 (*T212*) and Thr-231 (*T231*) are the reported Pin1-binding sites. Amino acid sequences of tryptic peptides containing the major Cdk5 phosphorylation sites are indicated below. Tau mutants with Ala replacement at the Cdk5 phosphorylation sites used in this study are also shown. *B*, an autoradiograph of WT Tau and Ala mutants at Ser-202 and/or Thr-205 phosphorylated by Cdk5-p25. *C*, two-dimensional phosphopeptide map of WT Tau and Ala mutants at Ser-202 and/or Thr-205 phosphorylated by Cdk5-p25. Four spots, 1–4, were detected with Tau WT. The phosphorylation spots 4 and 2/3 correspond to Ser-235 and Ser-404, respectively (29, 39). *Arrowheads* indicate the spot including phospho-Ser-202 or phospho-Thr-205. *D*, Tau-4A does not bind to Pin1. Tau WT or Tau-4A was phosphorylated by Cdk5-p25, and their binding to Pin1 was examined by a GST-Pin1 pulldown assay (*Bound*). Input is shown in the *middle panel*, and GST-Pin1 is shown in the *lower panel* by CBB staining. *E*, affinity of Cdk5-phosphorylated Tau binding to Pin1. WT Tau phosphorylated by Cdk5-p25 was applied to a Pin1-bound sensor tip in a Biacore instrument as described under "Experimental Procedures." The Scatchard plot was obtained by plotting the resonance units (*RU*) at equilibrium (Req)/Tau concentration (μM) against resonance units. A straight line was drawn using the least squares method. The linear regression equation between Req and Req/Tau (μM) was: $Req = R_{max} - Req/Tau \times K_d$ (95% confidence interval for the regression coefficient, -1.53×10^{-4} to -0.67×10^{-4}, and the coefficient of determination was $r^2 = 0.96$). The calculated K_d value was $1.11 \pm 0.14 \times 10^{-4}$ M (±S.D.).

analysis (Fig. 3*C*). WT Tau phosphorylated by Cdk5-p25 is shown in Fig. 3*A*, which shows four major phosphorylation spots that are identical to our previous results (29, 39). We previously assigned each spot to its corresponding phosphorylation site, Ser-202 for spot 1, Ser-404 for spots 2 and 3, and Ser-235 for spot 4. To determine whether phospho-Thr-205 is included in the same peptide as phospho-Ser-202, the two-dimensional phosphopeptide pattern of Tau-S202A (Fig. 3*B*) was compared with that of WT Tau. Spot 1 was still detected (Fig. 3*C*, S202A). To identify the remaining phosphorylation site in spot 1, we generated a Tau-S202A/T205A mutant and subjected it to two-dimensional phosphopeptide map analysis after phosphorylation by Cdk5-p25. Spot 1 disappeared in the double mutant S202A/T205A (Fig. 3*C*). Detection of spot 1 in T205A (Fig. 3*C*) confirmed the phosphorylation of Ser-202. These results indicate that spot 1 is the phosphopeptide containing either phospho-Ser-202 or phospho-Thr-205. Thus, Thr-205 in addition to Ser-202, Ser-235, and Ser-404 can be phosphorylated by Cdk5-p25 in *in vitro*.

Pin1 Binds to Tau at Any of the Four Cdk5 Phosphorylation Sites—To see whether Pin1 binds to Cdk5 phosphorylation sites in Tau, we generated a Tau-4A mutant in which all four major Cdk5 phosphorylation sites at Ser-202, Thr-205, Ser-235, and Ser-404 were mutated to alanine. Although a slight upward shift remained, the Cdk5-dependent upward shift was largely abolished in Tau-4A (Fig. 3*D*, *lane 4*, *Input*), confirming that these four residues are the major Cdk5 phosphorylation sites. Cdk5-phosphorylated Tau-4A abolished the binding of Pin1 to Tau (Fig. 3*D*), demonstrating that Pin1 binds to Tau at Cdk5-mediated sites. Next, we determined the affinity of WT Tau phosphorylated by Cdk5-p25 binding to Pin1 using Biacore technology. The amount of Tau bound to a constant amount of GST-Pin1 in the sensor tip was measured as resonance units at five different concentrations of Tau (Fig. 3*E*). These experiments were performed in the presence of 0.1 M NaCl, the same concentration used for the GST binding assay. Under this condition, we did not observe the binding of unphosphorylated Tau to Pin1 (data not shown). In contrast, phosphorylated Tau did bind to Pin1, and the amount of bound Tau increased with rising Tau concentrations with a dissociation constant (K_d) of $1.11 \pm 0.14 \times 10^{-4}$ M (Fig. 3*E*).

To identify the Pin1-binding sites conclusively, we constructed four triple alanine (3A) mutants of Tau by adding back Ser-202 (Tau-S202–3A), Thr-205 (Tau-T205–3A), Ser-235 (Tau-S235–3A), or Ser-404 (Tau-S404–3A) to Tau-4A (Fig. 3*A*, *lower panel*). Consistent with the idea that Cdk5 phosphorylates Tau mainly at Ser-202, Thr-205, Ser-235, and Ser-404, all of the 3A mutants were phosphorylated by Cdk5 to a similar extent, exhibiting about one-third of WT Tau phosphorylation (Fig. 4*A*). Moreover, Tau that was mutated at all four sites (Tau-4A) acted as a poor substrate for Cdk5. All four 3A mutants bound to Pin1 in a phosphorylation-dependent manner (Fig. 4*B*, *Bound*), indicating that Pin1 can recognize and bind to any of the major Cdk5-mediated sites including Ser-202, Thr-205, Ser-235, and Ser-404.

We wondered whether there might be differences between the binding strength of the individual mutants, and hence we compared their site-specific binding to Pin1 using Biacore technology. The protein concentration and phosphorylation were adjusted carefully in the Tau-3A mutants. When the extent of phosphorylation was the same, Tau-Ser202–3A and Tau-Thr205–3A showed slightly greater binding than did Tau-Ser235–3A and Tau-Ser404–3A (Fig. 4*C*). We observed similar results with three different preparations of Tau but could not derive reliable K_d values at the respective sites probably because of the relatively weak binding affinity.

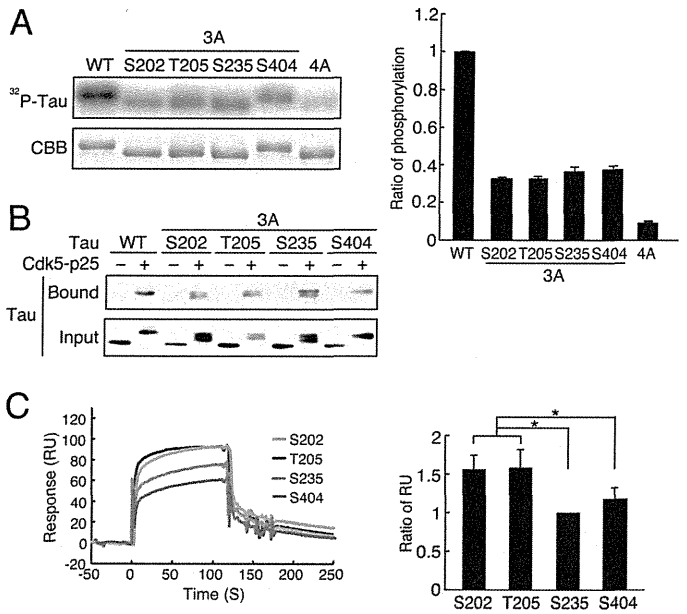

FIGURE 4. **Tau with a single phosphorylation at any site of Ser-202, Thr-205, Ser-235, or Ser-404 binds to Pin1 after phosphorylation by Cdk5-p25.** *A*, phosphorylation of Tau-3A mutants together with Tau WT and Tau-4A by Cdk5-p25. Tau WT and mutants at 0.1 mg/ml were phosphorylated by Cdk5-p25 in the presence of 0.1 mM [γ-^{32}P]ATP for 2 h at 35 °C. The extent of phosphorylation (*right panel*) was measured with an image analyzer (*left panel*, *^{32}P-Tau*) followed by normalization with Tau protein (*left panel*, *CBB*). *B*, the binding of phospho-Tau-3A mutants to Pin1. After phosphorylation with (+) or without (−) Cdk5-p25, the WT Tau or Tau-3A mutants were subjected to a GST-Pin1 pulldown assay. Tau was detected by immunoblotting with Tau5. *C*, binding of Cdk5-phosphorylated Tau-3A to Pin1 was measured on a Biacore instrument. Tau-3A mutants were phosphorylated by Cdk5-p25 followed by measurement of the amount bound to Pin1 measured on a Biacore instrument. The binding profiles are shown as resonance units (*RU*) in the *left panel*, and the relative ratio of each Tau-3A bound to Pin1 is shown in the *right panel* (mean ± S.E. (*error bars*); $n = 4$; *, $p < 0.05$).

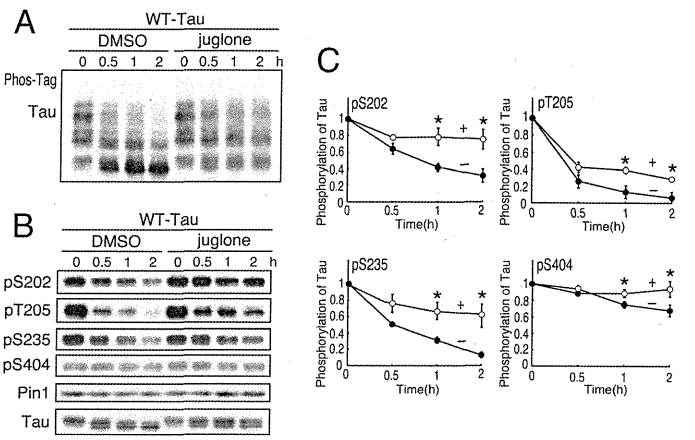

FIGURE 5. **Effects of Pin1 on dephosphorylation of Tau at Cdk5 phosphorylation sites.** *A*, the extracts of COS-7 cells expressing Tau and Cdk5-p25 were incubated with (+) or without (−) 5 μM juglone at 35 °C for the times indicated. Phosphorylation of Tau was examined by immunoblotting with anti-human Tau antibody after Phos-tag SDS-PAGE (*A*) or with phosphospecific antibodies against Ser-202 (*pS202*), Thr-205 (*pT205*), Ser-235 (*pS235*), or Ser-404 (*pS404*) after Laemmli SDS-PAGE (*B*). *C*, the rate of dephosphorylation at each Cdk5 phosphorylation site is shown as a comparison between the immunoblotting before (0 h) and after incubation (0.5, 1, or 2 h) in *B*. The results are expressed as mean ± S.E. (*error bars*) ($n = 3$; *, $p < 0.05$).

Effects of Pin1 on Dephosphorylation at Cdk5-mediated Tau Phosphorylation Sites—Pin1 increases dephosphorylation of Tau at Thr-231 (34, 38, 40). Although we have reported the increased dephosphorylation of Cdk5-phosphorylated Tau in rat brain extract (39), we did not examine the sites. We next tried to identify the sites for which dephosphorylation can be facilitated by Pin1. Tau was phosphorylated in COS-7 cells by co-expression of Cdk5 and p25 and subsequently dephosphorylated in cell extracts in the presence or absence of the Pin1 inhibitor juglone (52). To detect the complete phosphorylation state of Tau at a glance, we used Phos-tag SDS-PAGE in which the phosphorylated proteins are separated according to their phosphorylation states. WT Tau was separated into four major bands and many minor bands, indicating varied phosphorylation states in COS-7 cells. Incubation of the cell extract increased the electrophoretic mobility of Tau due to its dephosphorylation. Juglone delayed the mobility shift of Tau, indicating a decreased rate of Tau dephosphorylation (Fig. 5*A*).

We then tried to identify which sites were affected by juglone by immunoblotting with phosphospecific antibodies to Ser-202, Thr-205, Ser-235, or Ser-404 (Fig. 5*B*). Juglone decreased the dephosphorylation rate of Tau at any of the four sites (Fig. 5*C*). Consistent with our previous results (39), the dephosphorylation rate was slowest at Ser-404, although the rate was additionally reduced by juglone. Addition of Pin1 increased the rate of downward shift and Tau dephosphorylation (supplemental Fig. 3), although this effect was minor compared with Pin1 inhibition by juglone. To rule out the possibility that juglone inhibited protein phosphatase directly, we examined the effect of juglone on PKA-dependent Tau phosphorylation. Contrary to Cdk5 phosphorylation of Tau that was inhibited by juglone, PKA phosphorylation of Tau was not affected by juglone (supplemental Fig. 4). These results suggest that Pin1 stimulates the dephosphorylation of Tau at the Cdk5-mediated sites Ser-202, Thr-205, Ser-235, and Ser-404.

Binding of Cdk5-phosphorylated FTDP-17 Mutant Tau to Pin1—FTDP-17 Tau mutants are abnormally phosphorylated in the brains of FTDP-17 patients and in the brains of FTDP-17 mouse models (2–5, 25). However, it is not known how the Tau hyperphosphorylation is induced in FTDP-17. It is reported that Pin1 is reduced in AD brains (40). We examined Pin1 expression in one FTDP-17 patient and control brains but could not detect a change in Pin1 level (supplemental Fig. 5). Then we compared Pin1 in P301L transgenic mouse brains before and after appearance of pathological lesions. There was no difference between WT and P301L mouse brains at 3 months and in P301L mouse brains between 3 and 12 months (Fig. 6*A*). These results suggest that changes in Pin1 expression are not the underlying cause for Tau hyperphosphorylation in FTDP-17.

Tau-P301L and -R406W mutants are more resistant to Pin1-dependent dephosphorylation by PP2A compared with WT Tau (39). We suspected that the binding ability of Cdk5-phosphorylated Tau-P301L or -R406W to Pin1 might be weaker than that of WT Tau. Tau-P301L and -R406W were phosphorylated *in vitro* by Cdk5-p25 and subjected to a Pin1 binding assay. Both P301L and R406W Tau bound to Pin1 to the same extent as did WT Tau in the presence of 0.1 M NaCl when the phosphorylation levels were adjusted carefully (Fig. 6*B*). We then increased the concentration of NaCl in the binding buffer to reduce the binding (53). The amount of Tau bound to Pin1

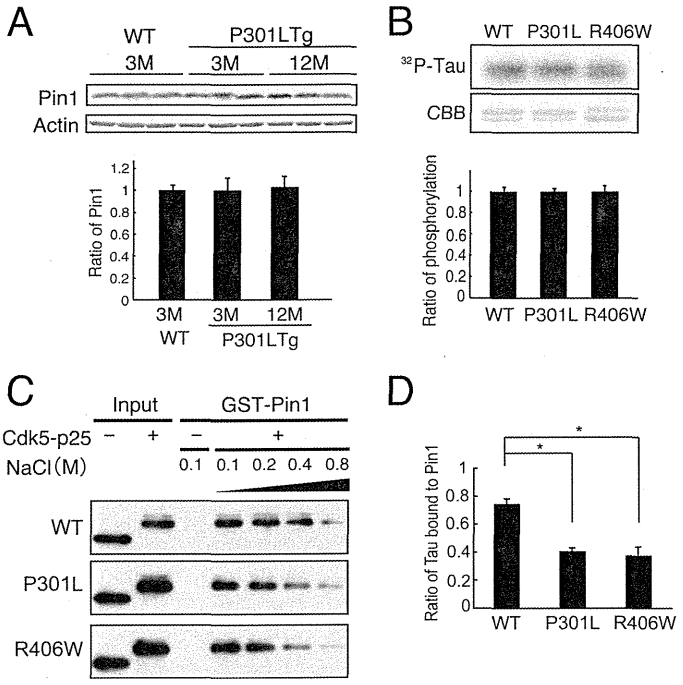

FIGURE 6. **Binding of Cdk5-phosphorylated FTDP-17 mutants to Pin1.** *A*, levels of Pin1 in P301L transgenic mouse brains. Pin1 was probed in whole brain lysates of wild-type mouse at 3 months and P301L transgenic (*Tg*) mouse at 3 and 12 months by immunoblotting. Actin is the loading control. Quantification is shown below. *B*, WT Tau and FTDP-17 Tau mutants P301L and R406W were phosphorylated by Cdk5-p25 in the presence of 0.1 mM [γ-^{32}P]ATP for 1.5 h at 35 °C. Phosphorylation of Tau was detected by autoradiography after SDS-PAGE (*^{32}P-Tau*) and quantified with an image analyzer (*lower panel*). The relative ratio is expressed against Tau WT after normalization with Tau protein (mean ± S.E. (*error bars*), $n = 3$). *C*, the binding of phospho-Tau P301L or R406W to Pin1. Tau-P301L or Tau-R406W was phosphorylated by Cdk5-p25 (+) and then subjected to a GST pulldown assay in the presence of increasing concentrations of NaCl from 0.1 to 0.8 M. Input is shown in the *left two lanes*. *D*, Tau bound to Pin1 in the presence of 0.4 M NaCl was expressed as the percent ratio against the binding in the presence of 0.1 M NaCl. The results are expressed as mean ± S.E. (*error bars*) ($n = 3$; *, $p < 0.05$).

decreased with increasing NaCl concentration (Fig. 6*C*). The ratio of Tau bound to Pin1 at 0.4 M NaCl was expressed relative to the amount of Tau bound to Pin1 in the presence of 0.1 M NaCl (Fig. 6*D*). The ratio was 41 ± 2.1% for P301L and 38 ± 6.2% for R406W, which were much lower than the 75 ± 3.4% for WT Tau. These results suggest that the affinity of Pin 1 binding to Tau carrying the FTDP-17 mutation P301L or R406W is slightly weaker than that to WT Tau.

DISCUSSION

In this study, we investigated the interaction of Pin1 with Cdk5-phosphorylated Tau and the effect on dephosphorylation at Cdk5 phosphorylation sites. Pin1 binds to Tau phosphorylated by Cdk5-p25 at any of its major phosphorylation sites, Ser-202, Thr-205, Ser-235, and Ser-404. The binding was slightly stronger to phospho-Ser-202 and -Thr-205 than to phospho-Ser-235 and -Ser-404. Pin1 facilitated the dephosphorylation of Tau at any of these sites. These are all abnormal phosphorylation sites found in AD (1, 2, 49). The FTDP-17 mutant Tau, P301L or R406W, showed slightly weaker binding to Pin1 than did WT Tau. These results support the idea that reduced Pin1-dependent dephosphorylation may underlie Tau hyperphosphorylation in tauopathies.

Phospho-Thr-212 and -Thr-231 were the only sites that had been previously mapped as Pin1-interacting sites in Tau (38, 40, 41, 54). Phospho-Thr-231 was first identified by an ELISA as a site among many synthetic phospho-Tau peptides (40). Phospho-Thr-212 was subsequently found to be another Pin1-binding site among GSK3β phosphorylation sites (41). Although the latter authors suggested that Thr-212 and Thr-231 are not unique as Pin1-binding sites based on the observation that Tau mutants at Thr-212 and Thr-231 still bound to Pin1 after phosphorylation in COS-7 cells (41), no other sites have been reported. We show here that there are at least four additional Pin1-binding phosphorylation sites in Tau at Ser-202, Thr-205, Ser-235, and Ser-404.

The binding of Pin1 to Tau at the Alzheimer-related phosphorylation site AT8, whose epitope is generated by phosphorylation of Tau at sites including Ser-202 and Thr-205 (55, 56), has been reported recently in rat cortical neurons (57); this finding is consistent with our present results. However, we do not know why these sites were not detected as Pin1-binding sites in previous work. It might be simply that no study has focused on Cdk5 phosphorylation sites, but we think there might be some mismatching between the protein kinases used and the phosphorylation sites examined. There are 16 (Ser/Thr)-Pro sequences in the longest isoform of Tau (2, 8, 10), many of which are phosphorylated distinctly and with an overlap by different PDPKs and are not necessarily phosphorylated stoichiometrically. Some of them are minor phosphorylation sites that can be detected only with highly sensitive phospho-specific antibodies. In the present study, we used Cdk5-p25, which has a substrate specificity similar to that of Cdk1 toward Tau (11, 50, 51). Having determined all major Cdk5 phosphorylation sites by a combination of phosphopeptide mapping and site-specific mutagenesis, we have shown that all major Cdk5 phosphorylation sites are also newly identified Pin1-binding sites. Extending this approach to other (Ser/Thr)-Pro sites could identify more Pin1-binding sites.

The dissociation constant K_d of Pin1 to Cdk5-phosphorylated full-length Tau was measured as $1.11 \pm .0.14 \times 10^{-4}$ M using Biacore technology. Two different K_d values have been reported for the binding between Pin1 and phosphorylated Tau or a phosphorylated Tau peptide: ~40 nM with the phospho-Thr-231 peptide when measured by an ELISA (40) and $3.8 \pm 1.0 \times 10^{-4}$ M at phospho-Thr-231 or $1.0 \pm 0.3 \times 10^{-4}$ M at phospho-Thr-212 by NMR (41). Our K_d value is close to the values measured by NMR. Furthermore, a similar K_d value, $\sim 1 \times 10^{-4}$ M, was reported for Csc25, a well known Pin1-binding protein (58). This K_d is relatively weak compared with many other protein-protein interactions. Nevertheless, GST pulldown assay worked well for both Cdc25 and Tau (59). The affinity of phospho-(Ser/Thr)-Pro sequences for Pin1 appears to be affected by various experimental conditions including the methods of measurement, the ionic strength of the solution, the number of phosphorylation sites, the use of phosphopeptides *versus* phosphorylated full-length proteins, and the WW domain of Pin1 *versus* full-length Pin1. We used phosphorylated full-length Tau instead of phosphopeptides, which may explain the low binding affinity. However, the weak affinity measured *in vitro* does not necessarily mean that the binding

does not occur in cells. Tau is highly concentrated in the vicinity of microtubules. Furthermore, *in vivo* Tau, particularly in brains with tauopathy, is phosphorylated at multiple (Ser/Thr)-Pro sites by multiple PDPKs, which may increase the binding affinity for Pin1. When highly phosphorylated, Tau may become a better target for Pin1, which may act on highly phosphorylated Tau in predisease conditions to prevent further phosphorylation. In other words, decreased Pin1 activity could be a consequence of Tau hyperphosphorylation. It has been reported that Pin1 is reduced in AD brains (40). We also examined the Pin1 level in an FTDP-17 brain and P301L transgenic mouse brains but could not detect differences between normal and patient or transgenic mouse brains (Fig. 6*A* and supplemental Fig. 5). We think that there must be other unknown factors that reduce the Pin1 activity in FTDP-17 brains.

The binding affinity also depends on the phospho-(Ser/Thr)-Pro sequences. For example, Smad2/3 has four Pin1-binding (Ser/Thr)-Pro sequences in the linker region, which can be phosphorylated by Cdk and MAPK family members but with strong binding at only one site (60, 61). In the case of Tau, phospho-Thr-212 has a lower K_d than phospho-Thr-231 (41, 54). We also observed here that the Cdk5 phosphorylation sites phospho-Ser-202 and -Thr-205 showed slightly stronger binding to Pin1 than did phospho-Ser-235 and -Ser-404. However, the correlation between Pin1 binding and dephosphorylation is not clear. The phosphorylation site grasped by the WW domain can be attacked by peptidylprolyl isomerase activity in the same Pin1 molecule (36, 37). Ser-202 with strong binding to Pin1 was dephosphorylated faster than was the weaker Ser-404 binding site. However, Ser-235, the weakest binding site, was dephosphorylated as fast as the stronger binding site Ser-202. By contrast, Pin1-binding sites are not always the sites whose dephosphorylation is stimulated by Pin1. It has been reported that peptidylprolyl isomerase catalyzes a different phosphorylation site close to the WW domain-binding site when the target protein is phosphorylated at multiple sites (53, 54). Tau is a multiphosphorylated protein with many clusters of (Ser/Thr)-Pro sequences. Previous research has also identified hierarchical phosphorylation by which GSK3β phosphorylation is facilitated by priming the phosphorylation by Cdk5 or PKA (13, 42, 62, 63). For example, Ser-404 phosphorylation is thought to be a priming site for Ser-400 and Ser-396 phosphorylation by GSK3β. The binding of Pin1 to phospho-Ser-404 may stimulate isomerization and then dephosphorylation at the Ser-396 GSK3β phosphorylation site. A similar relationship has been observed between the Ser-235 Cdk5 site and the Thr-231 GSK3β site (64).

FTDP-17 mutant Tau is hyperphosphorylated in brains of patients, but it is not known why. The phosphorylation levels of several FTDP-17 Tau mutants are similar to those of WT Tau when examined in cultured cells or *in vitro* (26–29, 65). R406W Tau shows even less phosphorylation by Cdk5 (29) probably because of mutation of Arg-406 to Trp, which changes the site to an unfavorable Cdk5 target sequence, S^{404}PWH from S^{404}PRH. We showed previously that P301L and R406W mutants do not show Pin1 dependence in dephosphorylation at the Cdk5 phosphorylation sites (39). We thought that Pin1 might not recognize the P301L or R406W Tau mutant phosphorylated by Cdk5, but this turned out not to be the case. At a physiological salt concentration, Pin1 bound to Cdk5-phosphorylated P301L and R406W Tau to the same extent as did WT Tau. By contrast, the protein stability of P301L Tau, but not WT Tau, was decreased in Pin1 knockdown or knock-out neurons, suggesting that the P301L mutation affects the interaction of Tau with Pin1 (66). The binding of Pin1 to both P301L and R406W Tau was slightly weaker than that to WT Tau when the binding was measured in the presence of a higher salt concentration. The slight difference in the binding affinity might be increased in the cellular condition by an unidentified factor. Further detailed biochemical studies are required to understand the Pin1-dependent regulation of Tau phosphorylation.

We found that Pin1 binds to and stimulates dephosphorylation of Tau at Cdk5-mediated sites Ser-202, Thr-205, Ser-235, and Ser-404. All of these sites conform at least in part to well known Tau hyperphosphorylation epitopes in AD (Ser-202 and Thr-205 for AT8, Ser-235 for AT180, and Ser-404 for PHF1). An involvement of Pin1 in the Tau hyperphosphorylation in AD has been suggested (38), but the two Pin1-binding sites identified so far could not explain the many other abnormally phosphorylated Tau sites. Our results identify novel Pin1-binding phosphorylation sites in Tau and characterize them as Cdk5-specific sites. Therefore, thorough analysis of the remaining (Ser/Thr)-Pro sites phosphorylated by other PDPKs may indeed reveal to what extent Pin1 can contribute to abnormal Tau phosphorylation in tauopathies.

Acknowledgments—We thank Junichiro Suzuki and Yutaka Sato for statistical data analysis.

REFERENCES

1. Ballatore, C., Lee, V. M., and Trojanowski, J. Q. (2007) Tau-mediated neurodegeneration in Alzheimer's disease and related disorders. *Nat. Rev. Neurosci.* **8,** 663–672
2. Goedert, M., and Jakes, R. (2005) Mutations causing neurodegenerative tauopathies. *Biochim. Biophys. Acta* **1739,** 240–250
3. Hutton, M., Lendon, C. L., Rizzu, P., Baker, M., Froelich, S., Houlden, H., Pickering-Brown, S., Chakraverty, S., Isaacs, A., Grover, A., Hackett, J., Adamson, J., Lincoln, S., Dickson, D., Davies, P., Petersen, R. C., Stevens, M., de Graaff, E., Wauters, E., van Baren, J., Hillebrand, M., Joosse, M., Kwon, J. M., Nowotny, P., Che, L. K., Norton, J., Morris, J. C., Reed, L. A., Trojanowski, J., Basun, H., Lannfelt, L., Neystat, M., Fahn, S., Dark, F., Tannenberg, T., Dodd, P. R., Hayward, N., Kwok, J. B., Schofield, P. R., Andreadis, A., Snowden, J., Craufurd, D., Neary, D., Owen, F., Oostra, B. A., Hardy, J., Goate, A., van Swieten, J., Mann, D., Lynch, T., and Heutink, P. (1998) Association of missense and 5′-splice-site mutations in tau with the inherited dementia FTDP-17. *Nature* **393,** 702–705
4. Poorkaj, P., Bird, T. D., Wijsman, E., Nemens, E., Garruto, R. M., Anderson, L., Andreadis, A., Wiederholt, W. C., Raskind, M., and Schellenberg, G. D. (1998) Tau is a candidate gene for chromosome 17 frontotemporal dementia. *Ann. Neurol.* **43,** 815–825
5. Clark, L. N., Poorkaj, P., Wszolek, Z., Geschwind, D. H., Nasreddine, Z. S., Miller, B., Li, D., Payami, H., Awert, F., Markopoulou, K., Andreadis, A., D'Souza, I., Lee, V. M., Reed, L., Trojanowski, J. Q., Zhukareva, V., Bird, T., Schellenberg, G., and Wilhelmsen, K. C. (1998) Pathogenic implications of mutations in the tau gene in pallido-ponto-nigral degeneration and related neurodegenerative disorders linked to chromosome 17. *Proc. Natl. Acad. Sci. U.S.A.* **95,** 13103–13107
6. Allen, B., Ingram, E., Takao, M., Smith, M. J., Jakes, R., Virdee, K., Yoshida, H., Holzer, M., Craxton, M., Emson, P. C., Atzori, C., Migheli, A., Crowther, R. A., Ghetti, B., Spillantini, M. G., and Goedert, M. (2002)

Abundant tau filaments and nonapoptotic neurodegeneration in transgenic mice expressing human P301S tau protein. *J. Neurosci.* **22,** 9340–9351
7. Ikeda, M., Shoji, M., Kawarai, T., Kawarabayashi, T., Matsubara, E., Murakami, T., Sasaki, A., Tomidokoro, Y., Ikarashi, Y., Kuribara, H., Ishiguro, K., Hasegawa, M., Yen, S. H., Chishti, M. A., Harigaya, Y., Abe, K., Okamoto, K., St George-Hyslop, P., and Westaway, D. (2005) Accumulation of filamentous tau in the cerebral cortex of human tau R406W transgenic mice. *Am. J. Pathol.* **166,** 521–531
8. Hanger, D. P., Anderton, B. H., and Noble, W. (2009) Tau phosphorylation: the therapeutic challenge for neurodegenerative disease. *Trends Mol. Med.* **15,** 112–119
9. Morishima-Kawashima, M., Hasegawa, M., Takio, K., Suzuki, M., Yoshida, H., Watanabe, A., Titani, K., and Ihara, Y. (1995) Hyperphosphorylation of tau in PHF. *Neurobiol. Aging* **16,** 365–371
10. Johnson, G. V., and Stoothoff, W. H. (2004) Tau phosphorylation in neuronal cell function and dysfunction. *J. Cell Sci.* **117,** 5721–5729
11. Imahori, K., and Uchida, T. (1997) Physiology and pathology of tau protein kinases in relation to Alzheimer's disease. *J. Biochem.* **121,** 179–188
12. Plattner, F., Angelo, M., and Giese, K. P. (2006) The roles of cyclin-dependent kinase 5 and glycogen synthase kinase 3 in tau hyperphosphorylation. *J. Biol. Chem.* **281,** 25457–25465
13. Ishiguro, K., Takamatsu, M., Tomizawa, K., Omori, A., Takahashi, M., Arioka, M., and Uchida, T. (1992) Tau protein kinase I converts normal tau protein into A68-like component of paired helical filaments. *J. Biol. Chem.* **267,** 10897–10901
14. Dhavan, R., and Tsai, L. H. (2001) A decade of CDK5. *Nat. Rev. Mol. Cell Biol.* **2,** 749–759
15. Hisanaga, S., and Endo, R. (2010) Regulation and role of cyclin-dependent kinase activity in neuronal survival and death. *J. Neurochem.* **115,** 1309–1321
16. Patrick, G. N., Zukerberg, L., Nikolic, M., de la Monte, S., Dikkes, P., and Tsai, L. H. (1999) Conversion of p35 to p25 deregulates Cdk5 activity and promotes neurodegeneration. *Nature* **402,** 615–622
17. Asada, A., Yamamoto, N., Gohda, M., Saito, T., Hayashi, N., and Hisanaga, S. (2008) Myristoylation of p39 and p35 is a determinant of cytoplasmic or nuclear localization of active cyclin-dependent kinase 5 complexes. *J. Neurochem.* **106,** 1325–1336
18. Asada, A., Saito, T., and Hisanaga, S. (2012) Phosphorylation of p35 and p39 by Cdk5 determines the subcellular location of the holokinase in a phosphorylation-site-specific manner. *J. Cell Sci.* **125,** 3421–3429
19. Minegishi, S., Asada, A., Miyauchi, S., Fuchigami, T., Saito, T., and Hisanaga, S. (2010) Membrane association facilitates degradation and cleavage of the cyclin-dependent kinase 5 activators p35 and p39. *Biochemistry* **49,** 5482–5493
20. Kusakawa, G., Saito, T., Onuki, R., Ishiguro, K., Kishimoto, T., and Hisanaga, S. (2000) Calpain-dependent proteolytic cleavage of the p35 cyclin-dependent kinase 5 activator to p25. *J. Biol. Chem.* **275,** 17166–17172
21. Lee, M. S., Kwon, Y. T., Li, M., Peng, J., Friedlander, R. M., and Tsai, L. H. (2000) Neurotoxicity induces cleavage of p35 to p25 by calpain. *Nature* **405,** 360–364
22. Cruz, J. C., Tseng, H. C., Goldman, J. A., Shih, H., and Tsai, L. H. (2003) Aberrant Cdk5 activation by p25 triggers pathological events leading to neurodegeneration and neurofibrillary tangles. *Neuron* **40,** 471–483
23. Noble, W., Olm, V., Takata, K., Casey, E., Mary, O., Meyerson, J., Gaynor, K., LaFrancois, J., Wang, L., Kondo, T., Davies, P., Burns, M., Veeranna, Nixon, R., Dickson, D., Matsuoka, Y., Ahlijanian, M., Lau, L. F., and Duff, K. (2003) Cdk5 is a key factor in tau aggregation and tangle formation *in vivo*. *Neuron* **38,** 555–565
24. Piedrahita, D., Hernández, I., López-Tobón, A., Fedorov, D., Obara, B., Manjunath, B. S., Boudreau, R. L., Davidson, B., Laferla, F., Gallego-Gómez, J. C., Kosik, K. S., and Cardona-Gómez, G. P. (2010) Silencing of CDK5 reduces neurofibrillary tangles in transgenic Alzheimer's mice. *J. Neurosci.* **30,** 13966–13976
25. Lambourne, S. L., Sellers, L. A., Bush, T. G., Choudhury, S. K., Emson, P. C., Suh, Y. H., and Wilkinson, L. S. (2005) Increased tau phosphorylation on mitogen-activated protein kinase consensus sites and cognitive decline in transgenic models for Alzheimer's disease and FTDP-17: evidence for distinct molecular processes underlying tau abnormalities. *Mol. Cell. Biol.* **25,** 278–293
26. Matsumura, N., Yamazaki, T., and Ihara, Y. (1999) Stable expression in Chinese hamster ovary cells of mutated tau genes causing frontotemporal dementia and parkinsonism linked to chromosome 17 (FTDP-17). *Am. J. Pathol.* **154,** 1649–1656
27. Pérez, M., Lim, F., Arrasate, M., and Avila, J. (2000) The FTDP-17-linked mutation R406W abolishes the interaction of phosphorylated tau with microtubules. *J. Neurochem.* **74,** 2583–2589
28. Connell, J. W., Gibb, G. M., Betts, J. C., Blackstock, W. P., Gallo, J., Lovestone, S., Hutton, M., and Anderton, B. H. (2001) Effects of FTDP-17 mutations on the *in vitro* phosphorylation of tau by glycogen synthase kinase 3β identified by mass spectrometry demonstrate certain mutations exert long-range conformational changes. *FEBS Lett.* **493,** 40–44
29. Sakaue, F., Saito, T., Sato, Y., Asada, A., Ishiguro, K., Hasegawa, M., and Hisanaga, S. (2005) Phosphorylation of FTDP-17 mutant tau by cyclin-dependent kinase 5 complexed with p35, p25, or p39. *J. Biol. Chem.* **280,** 31522–31529
30. Wang, J. Z., Gong, C. X, Zaidi, T., Grundke-Iqbal, I., and Iqbal, K. (1995) Dephosphorylation of Alzheimer paired helical filaments by protein phosphatase-2A and -2B. *J. Biol. Chem.* **270,** 4854–4860
31. Sontag, E., Nunbhakdi-Craig, V., Lee, G., Bloom, G. S., and Mumby, M. C. (1996) Regulation of the phosphorylation state and microtubule-binding activity of Tau by protein phosphatase 2A. *Neuron* **17,** 1201–1207
32. Liang, Z., Liu, F., Iqbal, K., Grundke-Iqbal, I., Wegiel, J., and Gong, C. X. (2008) Decrease of protein phosphatase 2A and its association with accumulation and hyperphosphorylation of tau in Down syndrome. *J. Alzheimers Dis.* **13,** 295–302
33. Yamamoto, H., Hasegawa, M., Ono, T., Tashima, K., Ihara, Y., and Miyamoto, E. (1995) Dephosphorylation of fetal-tau and paired helical filaments-tau by protein phosphatases 1 and 2A and calcineurin. *J. Biochem.* **118,** 1224–1231
34. Zhou, X. Z., Kops, O., Werner, A., Lu, P. J., Shen, M., Stoller, G., Küllertz, G., Stark, M., Fischer, G., and Lu, K. P. (2000) Pin1-dependent prolyl isomerization regulates dephosphorylation of Cdc25C and tau proteins. *Mol. Cell* **6,** 873–883
35. Nakamura, K., Greenwood, A., Binder, L., Bigio, E. H., Denial, S., Nicholson, L., Zhou, X. Z., and Lu, K. P. (2012) Proline isomer-specific antibodies reveal the early pathogenic tau conformation in Alzheimer's disease. *Cell* **149,** 232–244
36. Lippens, G., Landrieu, I., and Smet, C. (2007) Molecular mechanisms of the phospho-dependent prolyl cis/trans isomerase Pin1. *FEBS J.* **274,** 5211–5222
37. Liou, Y. C., Zhou, X. Z., and Lu, K. P. (2011) Prolyl isomerase Pin1 as a molecular switch to determine the fate of phosphoproteins. *Trends Biochem. Sci.* **36,** 501–514
38. Liou, Y. C., Sun, A., Ryo, A., Zhou, X. Z., Yu, Z. X., Huang, H. K., Uchida, T., Bronson, R., Bing, G., Li, X., Hunter, T., and Lu, K. P. (2003) Role of the prolyl isomerase Pin1 in protecting against age-dependent neurodegeneration. *Nature* **424,** 556–561
39. Yotsumoto, K., Saito, T., Asada, A., Oikawa, T., Kimura, T., Uchida, C., Ishiguro, K., Uchida, T., Hasegawa, M., and Hisanaga, S. (2009) Effect of Pin1 or microtubule binding on dephosphorylation of FTDP-17 mutant tau. *J. Biol. Chem.* **284,** 16840–16847
40. Lu, P. J., Wulf, G., Zhou, X. Z., Davies, P., and Lu, K. P. (1999) The prolyl isomerase Pin1 restores the function of Alzheimer-associated phosphorylated tau protein. *Nature* **399,** 784–788
41. Smet, C., Sambo, A. V., Wieruszeski, J. M., Leroy, A., Landrieu, I., Buée, L., and Lippens, G. (2004) The peptidyl prolyl cis/trans-isomerase Pin1 recognizes the phospho-Thr212-Pro213 site on Tau. *Biochemistry* **43,** 2032–2040
42. Ishiguro, K., Sato, K., Takamatsu, M., Park, J., Uchida, T., and Imahori, K. (1995) Analysis of phosphorylation of tau with antibodies specific for phosphorylation sites. *Neurosci. Lett.* **202,** 81–84
43. Yamada, M., Saito, T., Sato, Y., Kawai, Y., Sekigawa, A., Hamazumi, Y., Asada, A., Wada, M., Doi, H., and Hisanaga, S. (2007) Cdk5-p39 is a labile complex with the similar substrate specificity to Cdk5-p35. *J. Neurochem.*

102, 1477–1487
44. Taoka, M., Ichimura, T., Wakamiya-Tsuruta, A., Kubota, Y., Araki, T., Obinata, T., and Isobe, T. (2003) V-1, a protein expressed transiently during murine cerebellar development, regulates actin polymerization via interaction with capping protein. *J. Biol. Chem.* **278,** 5864–5870
45. Laemmli, U. K. (1970) Cleavage of structural proteins during the assembly of the head of bacteriophage T4. *Nature* **227,** 680–685
46. Kinoshita, E., Kinoshita-Kikuta, E., Takiyama, K., and Koike, T. (2006) Phosphate-binding tag, a new tool to visualize phosphorylated proteins. *Mol. Cell. Proteomics.* **5,** 49–57
47. Hosokawa, T., Saito, T., Asada, A., Fukunaga, K., and Hisanaga, S. (2010) Quantitative measurement of *in vivo* phosphorylation states of Cdk5 activator p35 by Phos-tag SDS-PAGE. *Mol. Cell. Proteomics.* **9,** 1133–1143
48. Goedert, M., Spillantini, M. G., Potier, M. C., Ulrich, J., and Crowther, R. A. (1989) Cloning and sequencing of the cDNA encoding an isoform of microtubule-associated protein tau containing four tandem repeats: differential expression of tau protein mRNAs in human brain. *EMBO J.* **8,** 393–399
49. Lee, V. M., Goedert, M., and Trojanowski, J. Q. (2001) Neurodegenerative tauopathies. *Annu. Rev. Neurosci.* **24,** 1121–1159
50. Illenberger, S., Zheng-Fischhöfer, Q., Preuss, U., Stamer, K., Baumann, K., Trinczek, B., Biernat, J., Godemann, R., Mandelkow, E. M., and Mandelkow, E. (1998) The endogenous and cell cycle-dependent phosphorylation of tau protein in living cells: implications for Alzheimer's disease. *Mol. Biol. Cell* **9,** 1495–1512
51. Wada, Y., Ishiguro, K., Itoh, T. J., Uchida, T., Hotani, H., Saito, T., Kishimoto, T., and Hisanaga, S. (1998) Microtubule-stimulated phosphorylation of tau at Ser202 and Thr205 by cdk5 decreases its microtubule nucleation activity. *J. Biochem.* **124,** 738–746
52. Hennig, L., Christner, C., Kipping, M., Schelbert, B., Rücknagel, K. P., Grabley, S., Küllertz, G., and Fischer, G. (1998) Selective inactivation of parvulin-like peptidyl-prolyl cis/trans isomerases by juglone. *Biochemistry* **37,** 5953–5960
53. Daum, S., Fanghänel, J., Wildemann, D., and Schiene-Fischer, C. (2006) Thermodynamics of phosphopeptide binding to the human peptidyl prolyl cis/trans isomerase Pin1. *Biochemistry* **45,** 12125–12135
54. Smet, C., Duckert, J. F., Wieruszeski, J. M., Landrieu, I., Buée, L., Lippens, G., and Déprez, B. (2005) Control of protein-protein interactions: structure-based discovery of low molecular weight inhibitors of the interactions between Pin1 WW domain and phosphopeptides. *J. Med. Chem.* **48,** 4815–4823
55. Goedert, M., Jakes, R., and Vanmechelen, E., (1995) Monoclonal antibody AT8 recognises tau protein phosphorylated at both serine 202 and threonine 205. *Neurosci. Lett.* **189,** 167–169
56. Shahpasand, K., Uemura, I., Saito, T., Asano, T., Hata, K., Shibata, K., Toyoshima, Y., Hasegawa, M., and Hisanaga, S. (2012) Regulation of mitochondrial transport and inter-microtubule spacing by tau phosphorylation at the sites hyperphosphorylated in Alzheimer's disease. *J. Neurosci.* **32,** 2430–2441
57. Nykänen, N. P., Kysenius, K., Sakha, P., Tammela, P., and Huttunen, H. J. (2012) γ-Aminobutyric acid type A ($GABA_A$) receptor activation modulates tau phosphorylation. *J. Biol. Chem.* **287,** 6743–6752
58. Wintjens, R., Wieruszeski, J. M., Drobecq, H., Rousselot-Pailley, P., Buée, L., Lippens, G., and Landrieu, I. (2001) ^{1}H NMR study on the binding of Pin1 Trp-Trp domain with phosphothreonine peptides. *J. Biol. Chem.* **276,** 25150–25156
59. Crenshaw, D. G., Yang, J., Means, A. R., and Kornbluth, S. (1998) The mitotic peptidyl-prolyl isomerase, Pin1, interacts with Cdc25 and Plx1. *EMBO J.* **17,** 1315–1327
60. Nakano, A., Koinuma, D., Miyazawa, K., Uchida, T., Saitoh, M., Kawabata, M., Hanai, J., Akiyama, H., Abe, M., Miyazono, K., Matsumoto, T., and Imamura, T. (2009) Pin1 down-regulates transforming growth factor-β (TGF-β) signaling by inducing degradation of Smad proteins. *J. Biol. Chem.* **284,** 6109–6115
61. Matsuura, I., Chiang, K. N., Lai, C. Y., He, D., Wang, G., Ramkumar, R., Uchida, T., Ryo, A., Lu, K., and Liu, F. (2010) Pin1 promotes transforming growth factor-β-induced migration and invasion. *J. Biol. Chem.* **285,** 1754–1764
62. Pei, J. J., Grundke-Iqbal, I., Iqbal, K., Bogdanovic, N., Winblad, B., and Cowburn, R. F. (1998) Accumulation of cyclin-dependent kinase 5 (cdk5) in neurons with early stages of Alzheimer's disease neurofibrillary degeneration. *Brain Res.* **797,** 267–277
63. Michel, G., Mercken, M., Murayama, M., Noguchi, K., Ishiguro, K., Imahori, K., and Takashima, A. (1998) Characterization of tau phosphorylation in glycogen synthase kinase-3β and cyclin dependent kinase-5 activator (p23) transfected cells. *Biochim Biophys. Acta* **1380,** 177–182
64. Ishiguro, K., Kobayashi, S., Omori, A., Takamatsu, M., Yonekura, S., Anzai, K., Imahori, K., and Uchida, T. (1994) Identification of the 23 kDa subunit of tau protein kinase II as a putative activator of cdk5 in bovine brain. *FEBS Lett.* **342,** 203–208
65. DeTure, M., Ko, L. W., Easson, C., and Yen, S. H. (2002) Tau assembly in inducible transfectants expressing wild-type or FTDP-17 tau. *Am. J. Pathol.* **161,** 1711–1722
66. Lim, J., Balastik, M., Lee, T. H., Nakamura, K., Liou, Y. C., Sun, A., Finn, G., Pastorino, L., Lee, V. M., and Lu, K. P. (2008) Pin1 has opposite effects on wild-type and P301L tau stability and tauopathy. *J. Clin. Investig.* **118,** 1877–1889

Parkinsonism and Related Disorders 19 (2013) 15–20

Contents lists available at SciVerse ScienceDirect

Parkinsonism and Related Disorders

journal homepage: www.elsevier.com/locate/parkreldis

Analyses of the *MAPT*, *PGRN*, and *C9orf72* mutations in Japanese patients with FTLD, PSP, and CBS

Kotaro Ogaki [a], Yuanzhe Li [b], Masashi Takanashi [a], Kei-Ichi Ishikawa [a], Tomonori Kobayashi [d], Takashi Nonaka [e], Masato Hasegawa [e], Masahiko Kishi [f], Hiroyo Yoshino [b], Manabu Funayama [a,b], Tetsuro Tsukamoto [g], Keiichi Shioya [h], Masayuki Yokochi [i], Hisamasa Imai [a], Ryogen Sasaki [j], Yasumasa Kokubo [j], Shigeki Kuzuhara [k], Yumiko Motoi [a], Hiroyuki Tomiyama [a,c], Nobutaka Hattori [a,b,c,*]

[a] *Department of Neurology, Juntendo University School of Medicine, Tokyo, Japan*
[b] *Research Institute for Diseases of Old Age, Juntendo University School of Medicine, Tokyo, Japan*
[c] *Department of Neuroscience for Neurodegenerative Disorders, Juntendo University School of Medicine, Tokyo, Japan*
[d] *Department of Neurology, Fukuoka University School of Medicine, Fukuoka, Japan*
[e] *Department of Neuropathology and Cell Biology, Tokyo Metropolitan Institute of Medical Science, Tokyo, Japan*
[f] *Department of Internal Medicine, Division of Neurology, Sakura Medical Center, Toho University, Sakura, Japan*
[g] *Department of Neurology, Numazu Rehabilitation Hospital, Numazu, Japan*
[h] *Department of Neurology, National Hospital Organization Miyazaki Higashi Hospital, Miyazaki, Japan*
[i] *Department of Neurology, Tokyo Metropolitan Health and Medical Treatment Corp., Ebara Hospital, Tokyo, Japan*
[j] *Department of Neurology, Mie University Graduate School of Medicine, Tsu, Mie, Japan*
[k] *Department of Medical Welfare, Faculty of Health Science, Suzuka University of Medical Science, Suzuka, Mie, Japan*

ARTICLE INFO

Article history:
Received 26 April 2012
Received in revised form
16 June 2012
Accepted 19 June 2012

Keywords:
MAPT
PGRN
C9orf72
De novo
Abnormal eye movements

ABSTRACT

Background: Mutations in the microtubule associated protein tau (*MAPT*) and progranulin (*PGRN*) have been identified in several neurodegenerative disorders, such as frontotemporal lobar degeneration (FTLD), progressive supranuclear palsy (PSP), and corticobasal syndrome (CBS). Recently, *C9orf72* repeat expansion was reported to cause FTLD and amyotrophic lateral sclerosis (ALS). To date, no comprehensive analyses of mutations in these three genes have been performed in Asian populations. The aim of this study was to investigate the genetic and clinical features of Japanese patients with *MAPT*, *PGRN*, or *C9orf72* mutations.

Methods: *MAPT* and *PGRN* were analyzed by direct sequencing and gene dosage assays, and *C9orf72* repeat expansion was analyzed by repeat-primed PCR in 75 (48 familial, 27 sporadic) Japanese patients with FTLD, PSP, or CBS.

Results: We found four *MAPT* mutations in six families, one novel *PGRN* deletion/insertion, and no repeat expansion in *C9orf72*. Intriguingly, we identified a *de novo MAPT* p.S285R mutation. All six patients with early-onset PSP and the abnormal eye movements that are not typical of sporadic PSP had *MAPT* mutations. The gene dosages of *MAPT* and *PGRN* were normal.

Discussion: *MAPT* p.S285R is the first reported *de novo* mutation in a sporadic adult-onset patient. *MAPT* mutation analysis is recommended in both familial and sporadic patients, especially in early-onset PSP patients with these abnormal eye movements. Although *PGRN* and *C9orf72* mutations were rare in this study, the *PGRN* mutation was found in this Asian FTLD. These genes should be studied further to improve the clinicogenetic diagnoses of FTLD, PSP, and CBS.

1. Introduction

Mutations in the microtubule-associated protein tau (*MAPT*) and the progranulin (*PGRN*) genes have been identified in families with frontotemporal dementia and parkinsonism linked to chromosome 17 [1–3]. Recently, two studies reported that the expansion of a noncoding GGGGCC hexanucleotide repeat in the *C9orf72* gene is

* Corresponding author. Department of Neurology, Juntendo University School of Medicine, 2-1-1 Hongo, Bunkyo, Tokyo 113-8421, Japan. Tel.: +81 3 5802 1073; fax: +81 3 5800 0547.
E-mail address: nhattori@juntendo.ac.jp (N. Hattori).

1353-8020/$ – see front matter © 2012 Published by Elsevier Ltd.
http://dx.doi.org/10.1016/j.parkreldis.2012.06.019

a major cause of both frontotemporal lobar degeneration (FTLD) and amyotrophic lateral sclerosis (ALS) [4,5].

Each of these genes can be associated with multiple clinical entities. Patients with *MAPT* mutations may receive diagnoses of frontotemporal dementia (FTD), primary progressive aphasia (PPA), or progressive supranuclear palsy (PSP). Rarely, corticobasal syndrome (CBS) or FTD with ALS (FTD-ALS) may be manifested in these patients [6]. The clinical diagnoses of patients with *PGRN* mutations include FTD, PPA, and CBS [6]. *C9orf72* repeat expansion causes FTD, ALS, FTD-ALS [4,5], PPA [5,7], and CBS [8] phenotypes. Thus, due to the complicated and often overlapping genetic and phenotypic variability in these patients, an accurate diagnosis of these clinical entities before autopsy is often difficult for clinicians.

To date, few comprehensive screening studies of these three genes have been performed in Asian populations. The aims of this study are to characterize the roles of known and, more importantly, novel disease-causing genes and to investigate the genetic and clinical features of FTLD, PSP, and CBS patients with *MAPT*, *PGRN*, and *C9orf72* mutations. In this study, we also describe the abnormal eye movements that are generally not observed in sporadic PSP but occur in early-onset PSP patients bearing *MAPT* mutations.

2. Methods

2.1. Subjects

We studied 75 Japanese patients who were diagnosed with FTLD, PSP, and CBS with or without a family history of disease. FTLD was divided into three subclasses: behavioral variant FTD (bvFTD), FTD-ALS, and PPA. The clinical diagnoses were established according to the consensus criteria for FTD [9], PPA [10], PSP [11], and CBS [12]. The characteristics of the 75 analyzed patients (69 index patients) are shown in Table 1. This study was approved by the ethics committee of the Juntendo University School of Medicine. Each subject provided written informed consent. All of the subjects in the control cohort were Japanese individuals and were evaluated by neurologists to ensure that no subjects exhibited any clinical manifestations of neurodegenerative diseases.

2.2. Genetic analyses

For direct sequence analysis, each exon was amplified by polymerase chain reaction (PCR) using published primers for *MAPT* [13] and *PGRN* [2] in a standard protocol. Dideoxy cycle sequencing was performed using Big Dye Terminator chemistry (Applied Biosystems, Foster City, CA). These products were loaded into ABI310 and 3130 automated DNA sequence analyzers and analyzed with DNA Sequence Analysis software (Applied Biosystems). To provide a qualitative assessment of the presence of an expanded $(GGGGCC)_n$ hexanucleotide repeat in the *C9orf72* gene, we performed repeat-primed PCR as previously described [4]. The normal repeat number of the GGGGCC hexanucleotide was determined in all of the patients using genotyping primers, as previously described [4]. The PCR products were analyzed on an ABI3130 DNA Analyzer and visualized using Gene Mapper software (Applied Biosystems).

Table 1
The clinical diagnoses and characteristics of 75 patients (69 index patients).

Clinical phenotype	No.	% of total	% of Male	Mean (SD) AAO (range, years)	Familial	Sporadic
FTLD	38	50.7	39.5	57.1 (±12.4), 36–78	21	17
bvFTD	29	38.7	34.5	54.5 (±12.6), 36–78	18	11
FTD-ALS	2	2.7	100	67.5 (±1.5), 66–69	1	1
PPA	7	9.3	42.9	65.0 (±7.4), 58–77	2	5
PSP	25	33.3	68.0	59.8 (±13.0), 40–76	18	7
CBS	12	16.0	33.3	58.4 (±9.52), 40–71	9	3
Total	75	100	48.0	58.2 (±12.3), 36–78	48	27
Index patients	69	92.0	46.4	58.9 (±12.4), 36–78	42	27
Relatives	6	8	66.7	50.3 (±6.6), 44–61	6	0

FTLD = frontotemporal lobar degeneration.
bvFTD = behavioral variant frontotemporal dementia.
FTD-ALS = frontotemporal dementia with amyotrophic lateral sclerosis.
PPA = primary progressive aphasia; PSP = progressive supranuclear palsy.
CBS = corticobasal syndrome; SD = standard deviation; AAO = age at onset.

2.3. Multiplex ligation-dependent probe amplification (MLPA)

To confirm the gene dosages of *MAPT* and *PGRN*, we performed MLPA using the SALSA MLPA P275-B1 MAPT-PGRN kit (MRC-Holland, Amsterdam, The Netherlands). The DNA detection/quantification protocol was provided by the manufacturer. The products were quantified using the ABI3130 Genetic Analyzer and Gene Mapper v3.7 (Applied Biosystems). The kit contains 32 probes, including 13 *MAPT* probes (located in exons 1–13) and 5 *PGRN* probes (located in exons 1, 3, 6, 10, and 12) located within other genes on chromosome 17q21. The MLPA data were analyzed as described previously [14].

2.4. Exon-trapping analysis

To determine whether a novel *MAPT* mutation was pathogenic, we performed an exon-trapping analysis. We used a wild-type construct and constructs containing the novel *MAPT* p.S285R or the IVS10+3 intronic mutation [15]. The *MAPT* sequences included exon 10, 34 nucleotides of the upstream intronic sequence and 85 nucleotides of the downstream intronic sequence. The PCR products were subcloned into the splicing vector pSPL3 (Invitrogen, Carlsbad, CA), and exon trapping was performed as described previously [15].

2.5. Paternity testing

Microsatellite analysis with 10 markers (D2S293, D3S3521, D4S2971, D5S495, D6S16171, D7S2459, D8S1705, D16S430, D18S450, and D20S842) was performed in Patient 1 and his parents to confirm paternity.

2.6. TA cloning

The novel *PGRN* heterozygous deletion/insertion found in this study, *PGRN* p.G338RfsX23 (c.1012_1013delGGinsC), was confirmed by cloning the PCR products into the pCR4-TOPO Vector using the TOPO TA Cloning kit (Invitrogen) and sequencing the two haplotypes of the heterozygote.

3. Results

3.1. Results of MAPT analysis

3.1.1. Genetic and molecular analyses of MAPT

In this study, we identified nine patients with *MAPT* mutations from six families. Four heterozygous missense mutations in *MAPT*, p.L266V, p.N279K, p.N296N, and the novel p.S285R (Supplementary Fig. 1), were identified by direct sequencing. None of the 182 normal Japanese controls included in this study had the *MAPT* p.S285R. In addition, we examined the amino acid sequences of the MAPT protein in other species and found that the site of the p.S285R mutation was highly conserved (see Supplementary Fig. 2). The novel p.S285R mutation in *MAPT* was detected in Patient 1 but not in his parents (Fig. 1A and Supplementary Fig. 1). The parentage of this patient and the DNA authenticity were confirmed using a microsatellite panel (see Supplementary Table 1). These results suggest that p.S285R is a *de novo* mutation. To investigate whether the p.S285R mutation is pathogenic, we performed an exon-trapping analysis. The p.S285R mutation produced a marked increase in the splicing of exon 10 (Fig. 1B) and resulted in the overproduction of tau isoforms that contain 4-repeat tau, such as IVS10+3 [15]. These results indicate that the p.S285R mutation is a novel, *de novo* pathogenic mutation. Previously, p.L266V, p.N279K, and p.N296N had been reported as pathogenic mutations [16–18].

Table 2 lists the clinical features of all of the *MAPT*- and *PGRN*-positive patients in this study, and Supplementary Fig. 3 shows Pedigrees C, D, E, F, and G. The average age at disease onset of patients with a single heterozygous *MAPT* mutation was 42.3 ± 2.9 (range: 37–46) years. MLPA analysis showed no gene dosage abnormalities (multiplications or deletions) in *MAPT* in this cohort.